Identification of Fractured Basement Reservoir Using Integrated Well Data and Seismic Attributes: Case Study at Ruby Field, Northwest Java Basin*

Made Suardana[1], Ari Samodra[1], Arief Wahidin[1], and Mohammad Rachmat Sule[2]

Search and Discovery Article #20195 (2013)
Posted June 21, 2013

*Adapted from extended abstract prepared in conjunction with poster presentation at AAPG Annual Convention and Exhibition, Pittsburgh, Pennsylvania, May 19-22, 2013, AAPG©2013

[1]Exploration, PT, Pertamina EP, Jakarta, Indonesia (made.suardana@pertamina.com)
[2]Lecturer at Applied Geophysics Research Division, Faculty of Mining and Petroleum Engineering, Bandung Institute of Technology, Bandung, Indonesia

Abstract

Oil has been discovered in basement fractures in many fields in the Indonesian region, such as at Suban Field in South Sumatera Basin where basement fractures were one of the exploration targets. This study is identifies fractured basement reservoirs using integrated well data and seismic attributes in the Ruby Field, Northwest Java Basin. Four wells penetrated the basement rock, which is marble, from which hydrocarbon flowed. Fractures were detected in the basement rock which enhanced porosity and permeability allowing hydrocarbon production. Therefore, locating the distribution of fractures is of utmost importance for development of this area. Imaging data (FMI) interpretation can characterize the potential fractures or open fractures. FMI analysis indicated that the fractured basement has acted as a reservoir that is potentially charged by the nearest source rock. In order to better identify the faults and fractures at Ruby Field, a newly developed tool for fault mapping was applied. The Ant Track provides a powerful 3D automated technology for identifying and enhancing the complex faults which are responsible for the generation of natural fractures. The Ant Track map correlates very well with well data. For this reason, the Ant Track map can be used as a sophisticated method to track the distribution of potential fractures both laterally and vertically. Based on amplitude modeling, the lowest value of amplitude attributes, such as acoustic amplitude, sum amplitude, sum negative amplitude and minimum amplitude, are found to represent higher porositie distribution that might be related to fractures. The combination of well data (core and FMI), seismic attributes and Ant Track map analysis has successfully detected a potential open fractured basement reservoir northeast of MD-01 well.

Introduction

Fractured reservoirs are more difficult and expensive to evaluate than conventional reservoirs (Nelson, 1985), so a greater understanding of the fracture distribution and its relation with potential basement reservoirs may prove to be the key tool for improved exploration and production management of this hidden resource. To exploit this type of reservoir to the fullest, comprehensive study must be done, including determination of the distribution and orientation of fractures and possible migration and trap of hydrocarbon in the area. To develop an oil field with fractured reservoir, it is critical to know the distribution of faults and fractures, dimensions, geometry and genesis of the fractures, and especially the ages of fractures. How to identify the distribution and the orientation of the fracture is a difficult problem. Traditionally, fault and fractures can be identified by discontinuity events seen in seismic profiles. This research attempts to investigate the orientation and distribution of the faults and fractures using integrated well data (core and FMI) and seismic attributes methods. The image resolution of faults and fractures from seismic attributes will be enhanced using the Ant Track method. Finally, potential basement areas with possible open fractures filled with hydrocarbon can be mapped.

Geology of Northwest Java Basin

Northwest Java Basin is located north of the Java Volcanic Arc. About 300-400 km to the south of this basin is the collision arc between the Eurasian and Australian plates (Figure 1). Northwest Java Basin consists of the main epicenter basin, which includes the Jatibarang Sub-basin, Cipunegara Sub-basin, Arjuna Sub-basin and Ciputat Low (Figure 2). Ruby Field is located in the sub-basin of the Ciputat Low which is bounded by Rengasdengklok High on the east and Ciputat Deep on the west. Today, Northwest Java Basin belongs to a back arc basin, but the rifting process occurred during the Eocene in a different tectonic setting. Geologic evidence shows that this basin was a pull-apart basin due to dextral strike slip fault motion, with a north-south orientation of the main fault which is orthogonal to the subduction zone. The basin was formed due to the rifting process that involved thick continent crust (Pertamina, 2009, after Hamilton, 1979). Based on data from well MD-2 and tectonic stratigraphy analysis, about 200 m of basement was drilled. The basement is metamorphic rock consisting of marble and slate (S-types) with poor porosity, but some fractures indicated oil traces.

Petroleum System of the Ruby Field

The source rock of the Ruby field is shale in the Talang Akar Formation (TAF) and Pre-TAF. The main reservoirs in Ruby field are basement metasediments (marble or slate) which produced oil and gas from MD-01 well. The results of two DSTs in MD-01 are: DST-1 produced 3096 BOPD + 3.92 MMSCFD, and DST-2 showed 2901.9 BOPD + 2.813 MMSCFD. Open fractures were developed in basement metasediments with porosity ranging from 0.15% to 0.3 %, and a thicknessness of about 200 m. The seal of the metasediment was formed by discontinuity of open fractures, the hydrocarbon is trapped where open fractures are not connected with other fractures. Oil and gas migrated from Pre-TAF through carrier beds and faults until trapped. Besides carrier beds, the oil and gas also entered the basement below the Pre-TAF because of open fracture growth in the basement. Hydrocarbon is found trapped in basement in wells MD-01, MD-02 and MD-04 in the study area.

Basic Theory

A reservoir fracture is a naturally occurring macroscopic planar discontinuity in rock due to deformation or physical diagenesis (Nelson, 1985). The origin of the fracture system is postulated from data on fracture dip, morphology, strike (if available), relative abundance, and the angular relationship between fracture sets (Nelson, 1985). These data can be obtained from full-diameter cores (oriented or conventional) or the new imaging tools FMI and DSI Stoneley. Stearns and Friedman (1972) classified fractures based on genetic nature. There are tectonic fractures, regional fractures, contractional fractures, and surface-related fractures. Tectonic fractures are those whose origin can, on the basis of orientation, distribution, and morphology, be attributed to or associated with a local tectonic event. Nelson (1985) has observed that the majority of tectonic fractures in outcrop tend to be shear fractures (Figure 3). These fractures form in network with specific special relationships to folds and faults. Open fractures, as the name implies, possess no diagenetic material filling the width between the walls and fracture (Nelson, 1985). Such fractures are open conduits to fluid flow. Variance, which measures the degree of dissimilarity, is applied to enhance lateral changes of seismic data due to changes of geologic conditions (Sukmono, et al., 2006). The variance cube will show discontinuity parameters that reflect fault, fracture, unconformity or lithology distribution. Faults with detectable vertical throw are generally associated with a narrow zone of low similarity or high variance. Another attribute, the seismic amplitude generally is used to identify the following parameters: gas and fluid accumulation, gross lithology, gross porosity, channel and deltaic sandstones, specify type of reefs, unconformities, tuning effects and the changes in stratigraphic sequence (Figure 4).

Electrical and ultrasonic borehole images, along with conventional sonic logs can be used to characterize fracture systems. Electrical image methods, however, assume that all conductive fractures are open and can transmit fluids. In reality, the majority of fractured reservoirs flow hydrocarbons from only a few isolated fractures, or from a specific fracture “set” or “system”. A combination of image logs and acoustic logs can provide the detailed information needed to fully characterize fractures and other forms of high permeability geological flow conduits. The combination of these measurements allows a detailed analysis of fracture type (open, closed or plugged), fracture orientation, and most importantly the ability of individual open fractures and fracture sets to flow fluid.

The idea of Ant Track application is based on an algorithm called an ant colony optimization metaheuristic. This algorithm was developed by adapting the natural habit of ants when they are searching for food (Figure 5). They will go away from their nest, sometimes they meet the intersection and they must decide which route they will choose. They will locate the route by leaving pheromone on that route. Pheromone is a kind of hormone that is produced by ants to locate their route. The more frequently the route is used, the higher concentration of pheromone in that route. The next ant will follow the route that has the highest pheromone concentration.

Research Workflow

This research used two main types of data: well data (log data such as: GR, RHOB and Sonic) and 3D seismic data. The main workflow is shown in Figure 6. The principal of the Ant Track method is automatically re-picking the variance attributes which have the same character. This process will produce a new seismic cube called the Ant Track cube. The flow of the Ant Track process can be seen on Figure 7.

The advantages of using the Ant Track cube to interpret faults and fractures are: (1) the pattern of faults and fractures appears more explicitly than any other method (e.g. variance) so that the fault and fracture zones will be easy to interpreted manually or automatically, (2) filtering can be set to the pattern of fault or fracture zone by removing noise or patterns caused by lithology, (3) filtering can be set to the specific orientation of fractures, and (4) the Ant Track cube can be analyzed qualitatively or quantitatively.

Results and Interpretation

Rock cuttings from the MD-02 well are composed of dolomitic meta-limestone (90%), shale (5%), carbon material (4%), and sandstones (1%). Based on its texture and composition, this rock is classified as a marble. Some fractures in this rock can be seen in Figure 8.

In the FMI images, fractures are indicated as planes that have no significant displacement. They could be open fractures (with aperture), closed fractures (no aperture) or mineral clay-filled fractures (e.g. clays, calcite, anhydrite, pyrite, etc.). Here, fractures tend to occur as sine wave images and their dips are generally steeper than foliation dips. Open fractures have a conductive appearance on the image due to inclusion of conductive drilling mud. Mineralized or sealed fractures will have a resistive appearance if their filling material is resistive, such as calcite, quartz or anhydrite. Dipole Shear Sonic Induced (DSI) Stoneley fracture analysis was also carried out to determine permeable conductive fractures.

Another interpretation of conductive fractures at other depth intervals in the MD-02 well is shown in Figure 10. It is concluded that the average dominant orientation of conductive fractures or open fractures in both wells (MD-01 and MD-02) are between N340E and N30E, but the strike is dominantly north-south. This general orientation is in good agreement with the major fault strike (north-south) that formed this pull-apart basin (Figure 11). This result also supports the structural pattern and distribution of faults and fractures in Java that have been studied by Benyamin Sapiie and JAPEX (2006). They have measured the fault and fracture orientations based on basement outcrops (Figure 12). Especially in the Northwest Java Basin, the average fracture orientations in the basement are N340E-N30E. The fractures orientation is in good agreement with major fault strike. It can be concluded, then, that the fractures generated in the study area belong to the fault system. This type of fractures assumed that the fractures are distributed mostly near fault growth, i.e. faulting controlled the distribution of fractures. Figure 13 shows the indication of open fractures, energy loss and chevron patterns from DSI Stoneley data at different interval depths in MD-01 well. Potential fractures are identified with high fracture porosity, high energy loss and the indication of chevron pattern. The results indicate there are two potential fractures, first at interval 2730 m to 2775 m, and along interval 2820 to 2920 m. It is probably the 4000 BOPD production from marble reservoir in MD-01 came from the first interval.

Quality control of the fault interpretation is assessed by comparing the fault interpretation from amplitude slice, variance and Ant Track (Figure 14). The numbers of faults interpreted in variance are bigger and more accurate than in the amplitude slice (Figure 14b). Figure 14c is the result of Ant Track analysis, the resolution of the faults image is more explicit compared to the amplitude slice or the variance slice. Small faults that were not seen in variance slices have been successfully identified here, and even the fracture zone patterns are better defined.

Figure 15 shows Ant Track map slice at 2230 ms or about near the top of basement in MD-01 well. Many faults and probably fracture zones have been detected on the map. Faults, shown by bold red to blue color, are identified with high Ant Track value. The high values are due to

large fault offsets due to fault movement. Interpreted faults from Ant Track have orientations from NNW-SSE to NNE-SSW but mostly north-south. Fractures and fracture zones are shown by grey to red color, or the smallest value of Ant Tracking. The small values of Ant Track are due to a very small offset or displacement of rock due to fractures movement. Interpreted fractures have the same orientation as the faults, from NNW-SSE to NNE-SSW direction, with the average dominant fractures orientation of N340E-N30E as indicated by FMI. The increased resolution of the faults and fractures image has enabled the examination of fault intensity to detect the location of potential developed fractures by combining the Ant Track map with FMI data. The structure of the basement is shown by a time structure map in Figure 16.

During the Ant Track process, the closed fractures were filtered out and only open fractures were included from the FMI image. Figure 17 shows the process of obtaining the open fractures distribution from the Ant Track map. In this research, two trials of filtering were done. First, by including only the potential fractures from N340E-N60E, and second by including only the potential fractures from N340E-N30E. The results of the Ant Track map searching direction from N340E-N30E was more correlated with FMI data and so was chosen as the best result (Figure 17). The higher the correlation between the Ant Track result with the well data, the better the quality of the Ant Track map. Figure 18 shows good validation of the map with well data from the MD-01 and MD-02 wells. This Ant Track map was then used to map the distribution of open fractures in the study area.

Fractures are hardly detected in the seismic data. This is because the resolution of fractures usually cannot be resolved by seismic; however, distribution of fractures is probably related to porosity distribution and the porosities can be approximated by seismic attributes. This assumption starts with the relation between porosity and velocity (Figure 19): the contrast acoustic impedance between Pre-TAF and non-fractured top basement is stronger than between Pre-TAF with fractured top basement. Petrophysical modeling of amplitude versus depth was used to prove the assumption (Figure 19a). Based on the petrophysics modeling, some amplitude attributes were run to identify the distribution of higher porosities. Figure 20 shows that there are two decreased amplitudes in the seismic section, which is interpreted as developed fractures. The existence of fractures has decreased the amplitude of the top of the basement. To delineate the distribution of this anomaly laterally, we ran four seismic attributes. The first target to be delineated is the interval 2730-2775 m that contains many potential fractures with high fracture porosities (Figure 13). The attribute amplitude was run with a window of 5 ms above top of basement and 25 ms below of top basement. Figure 21 shows the results, with the distribution of higher porosities related to fracture distribution being identified by low amplitude values.

Figure 23 shows a 3D view location of potential fractures. There are abundant fractures detected between the MD-01 and MD-04 wells, with an especially high distribution of open fractures to the northeast of MD-01 well which flowed 4000 BOPD from fractured basement from the first interval during a DST. The potential open fractures basement is distributed around the MD-01 well (Figure 23) and has been successfully delineated by attribute analysis, and also supported by the Ant Track map. Because the distribution of the first interval of interest did not continuously develop deeper into the basement, horizontal drilling may be useful in this interval and trying to penetrate the fractures orthogonally to their strike for maximizing production.

The Ant Track map has showed a good result in tracking the distribution of potential fractures or open fractures. How do we know its quality? The validation of the Ant Track result is correlated to FMI data, and the correlation is quite good. Now the Ant Track map is correlated with well data, and especially from well data production. Figure 24 shows Ant Track map correlation with MD-01 well data. Ant Track map sliced

at numerous depths can map the distribution of fractures around the well, and that distribution is very well correlated with the well data. The map has detected the first interval (2726-2782 m) and second interval (2902-2920 m) which is flowing hydrocarbon from fractures. The map has also detected intervals with no production, between the first and second intervals at 2834 m. Figure 25 shows the Ant Track map is also well correlated with MD-04 well data. The Ant Track map can explain why top of basement is interpreted as tight with no porosity from rock sampling since it was predicted before drilling that the characteristic of top basement would be similar with top basement of MD-01 well which is not fractured. Ant Track map sliced at top basement (2726 m) has explained why no fractures are in the well. At a deeper depth of around 3200 m, well data has recorded oil flowing from fractured basement and the Ant Track map predicted more fractures at depths of 3180 m, 3201 m and 3205 m.

The results show that fracture distribution in the Ant Tract map is very well correlated with well data, so the Ant Tract map can be used to track both laterally and vertically open fractures which may be filled with hydrocarbon. The Ant Track map can be used by G&G in making drilling proposals to manage the deviation survey for optimal direction for horizontal drilling in order to penetrate the fractures orthogonally to strike so large fractures can be penetrated. Regarding the orientation of potential fractures in the study area, a horizontal well lateral from west to east is suggested for producing potential fractured basement reservoir northeast of the MD-01 well.

Conclusions and Recommendations

The petrographic report indicates that basement rock is marble, and fracture porosity is developed in the range of 0-1%. FMI analysis at MD-01 and MD-02 wells in the basement interval concludes that fault orientation is dominantly north-south, while open fractures are dominantly in the range of N340E to N30E. FMI analysis has enabled characterizing the factures in basement as reservoir that is potentially charged by hydrocarbon from the nearest source rock. The Ant Track map enhanced the resolution of fault and fracture images. Based on amplitude modeling, some amplitude attributes such as acoustic amplitude, sum amplitude, sum negative amplitude and minimum amplitude have been very helpful in tracing higher distribution of porosity in seismic associated with open fractures. In the study area, the Ant Track map is very well correlated with well data and proves a sophisticated method to track the distribution of fracture zones both laterally and vertically. The combination of FMI, seismic attribute and Ant Track analysis has successfully detected two open fractured basement reservoirs as prospects. They are located in the northwest and northeast parts of the study area. Because there is no well data to support the northwest area prospect, the prospect of potentially fractured basement reservoir to the northeast of MD-01 is a first priority to be drilled.

To prove the potential open fractured basement in the northwest, an exploration well should be drilled that will penetrate basement rock in the west of the study area. This research suggests the optimal orientation to drill horizontal wells is in a west-east direction, in order to produce more oil from potential fractured basement reservoir at the northeast of MD-01 well by penetrating the fractures orthogonally.

Selected References

Borland, W.H., R.E. Netherwood, S. Hutabarat, D. Juandi, L. Anis, H. Kurniawan, and R. Eyvazzadeh, 2001, Evaluation of Naturally Fractured Reservoirs In Indonesia Using Formation Imaging and Sonic Logs: Proceedings of Indonesia Petroleum Association 28th Annual Convention and Exhibition, v. 1, p. 458-497.

Fachri, M., 2001, Fault-Related Fracture Characterization: A Quantitative Approach in Naturally Fractured Reservoir Characterization: Proceedings Indonesia Petroleum Association 28th Annual Convention and Exhibition, v. 1, p. 500-512.

LAPI-ITB and Pertamina, 2008, Facies Distribution and Reservoir Quality of Syn-rift and Post-rift sediment Ciputat-Rengasdengklok Area: ITB, Final Report, Chapter 2, p. 1-3.

Landes, K.K., J.J. Amoruso, L.J. Charlesworth, F. Heany, and J. Lesperancep, 1960, Petroleum Resources in Basement Rocks: AAPG Bulletin, v. 44/10, p. 1682-1691.

P'an, C.H., 1982, Petroleum in Basement Rocks: AAPG Bulletin, v. 66/10, p. 1597-1643.

Randen, T., S.I. Pedersen, and L. Sonneland, 2001, Automatic extraction of fault surfaces from three-dimensional seismic data: Society of Exploration Geophysicists, 71st annual meeting; technical program, expanded abstracts with authors' biographies: SEG Annual Meeting Expanded Technical Program Abstracts with Biographies, v. 71, p. 551-554.

Nelson, R.A. 1985, Geologic Analysis of Naturally Fractured Reservoirs: Gulf Publishing Co. Book Division, p. 1-3.

Stearns, D.W., and M. Friedman, 1972, Reservoirs in Fractured Rock: AAPG Memoir, Stratigraphic oil and gas fields; Classification, Exploration Methods, and Case Histories, v. 16/10, p. 82-106.

Sukmono, S., D. Santoso, A. Samodra, W. Waluyo, and S. Tjiptoharsono, 2006, Integrating seismic attributes for reservoir characterization in Melandong Field, Indonesia: Leading Edge, v. 25/5, p. 532-538.

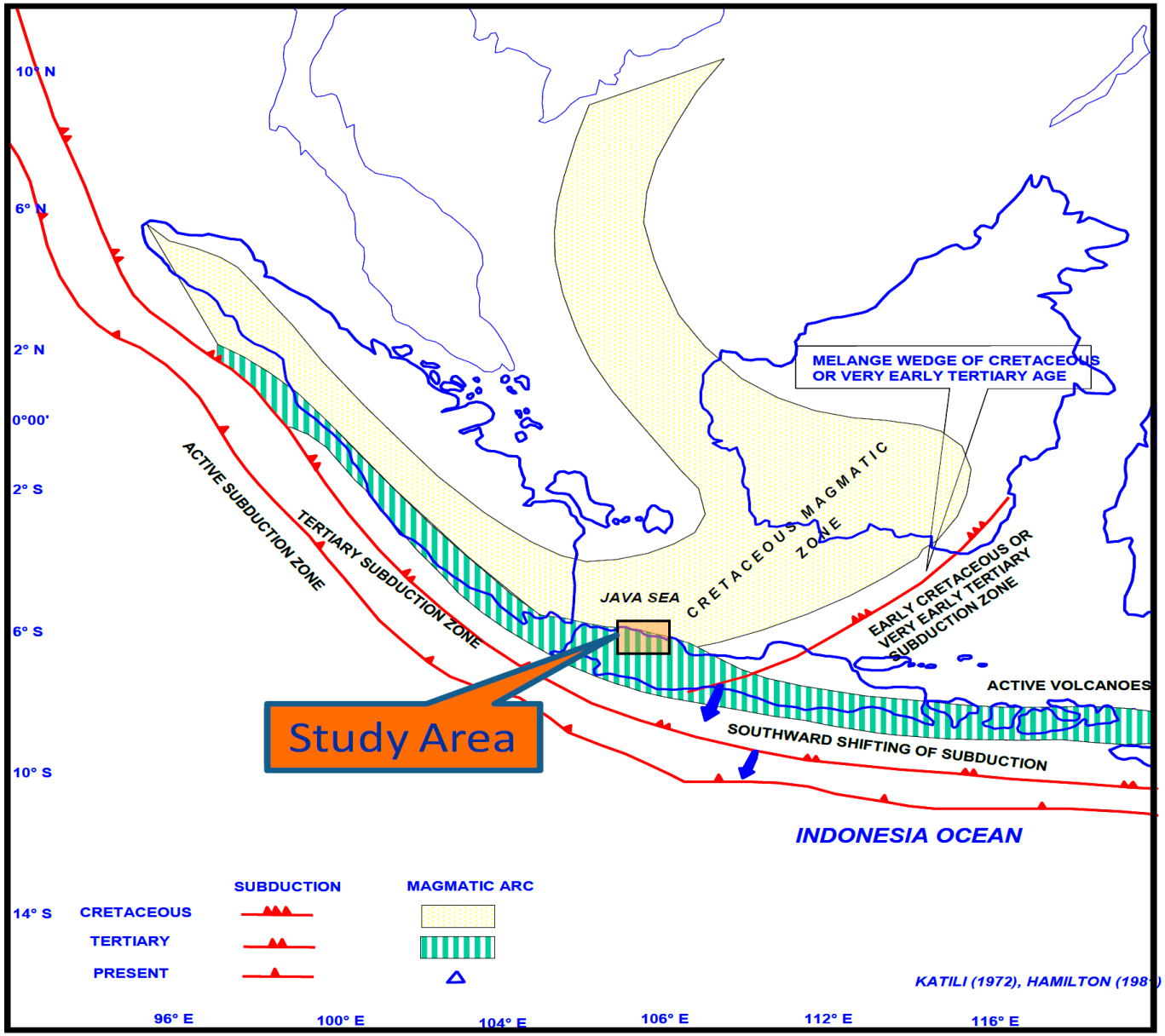

Figure 1. Tectonic setting of West Indonesia.

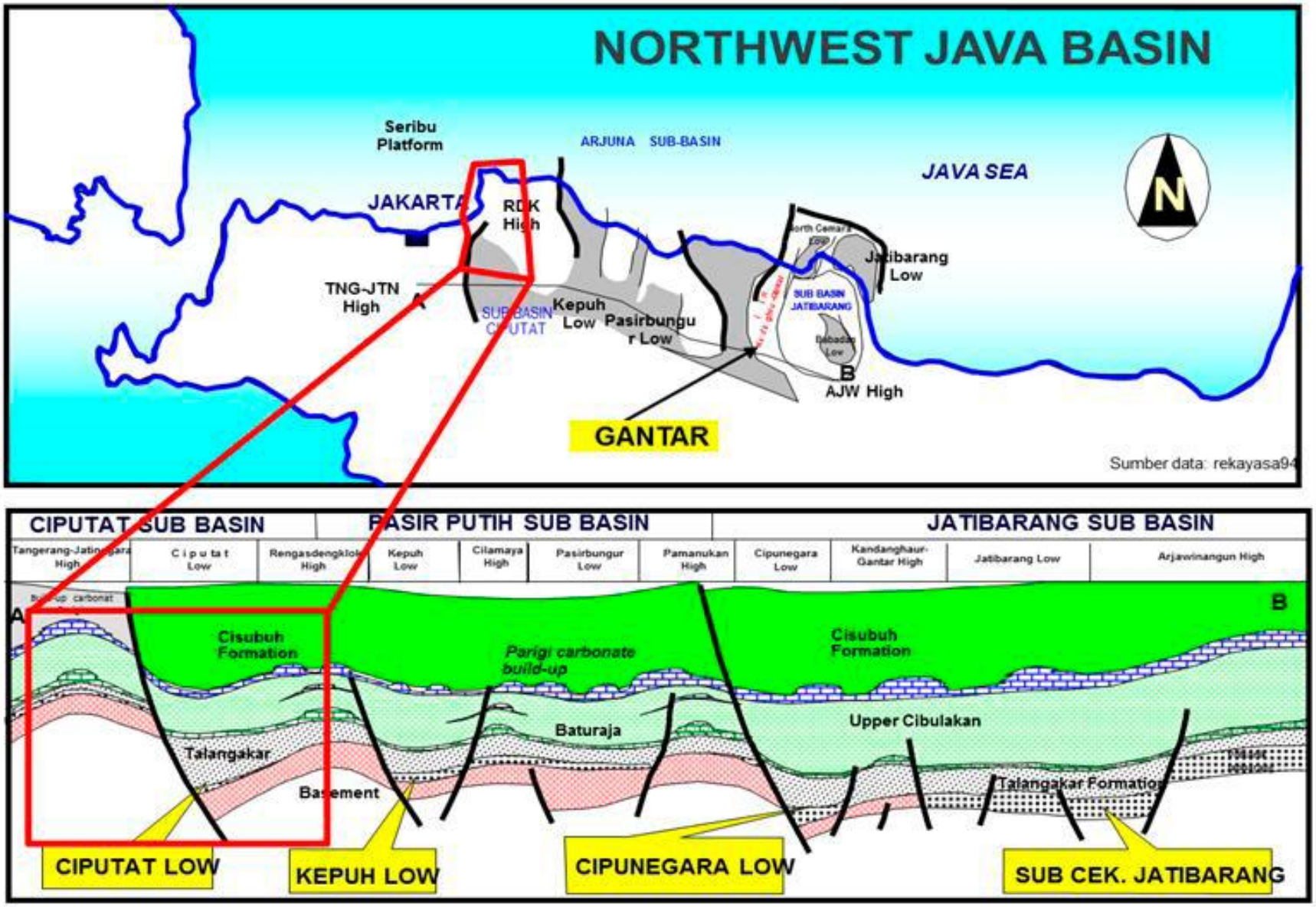

Figure 2. West-East cross ection of Northwest Java Basin.

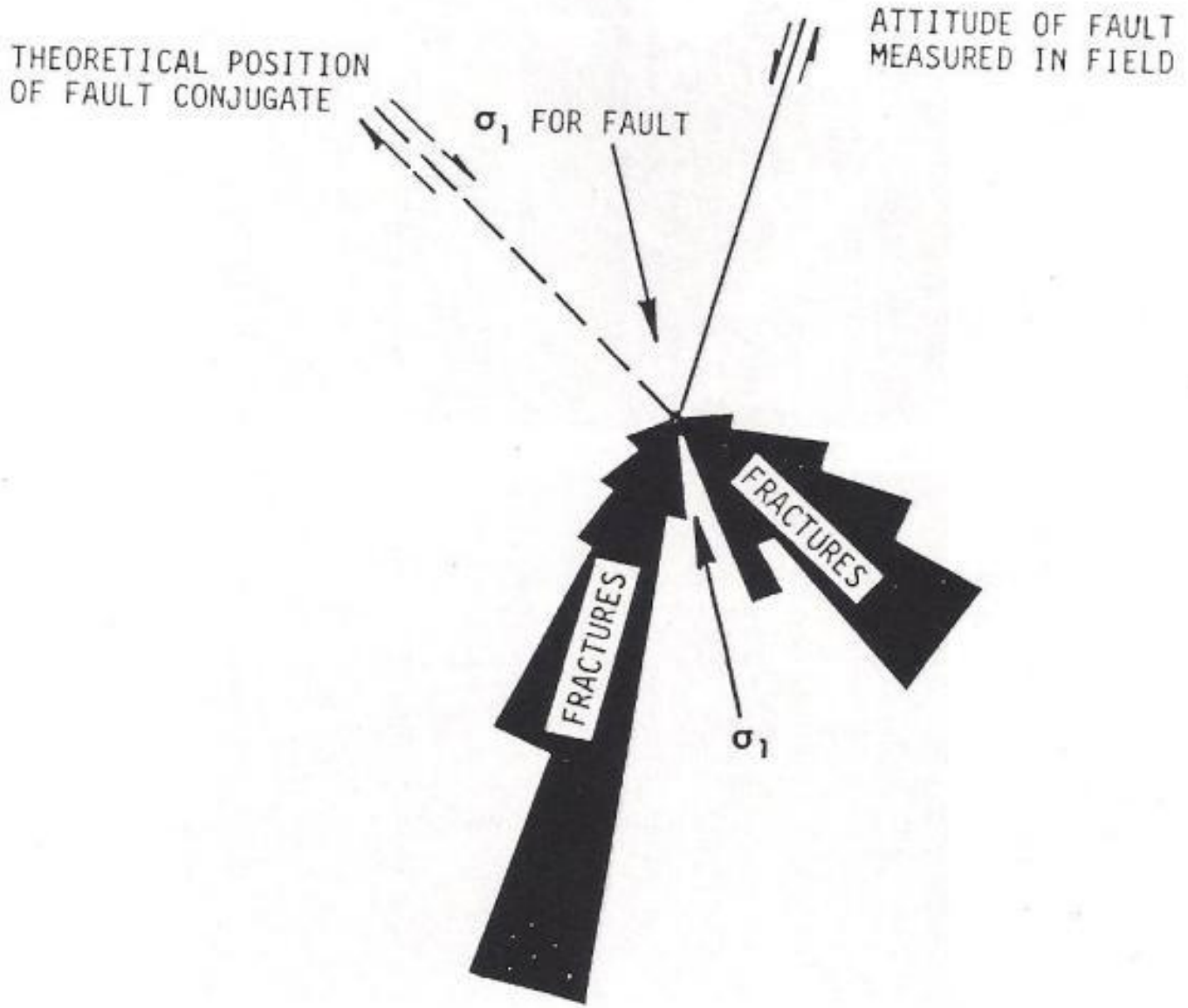

Figure 3. Rose diagram of shear fractures associated with normal fault. After Stearns (1986b).

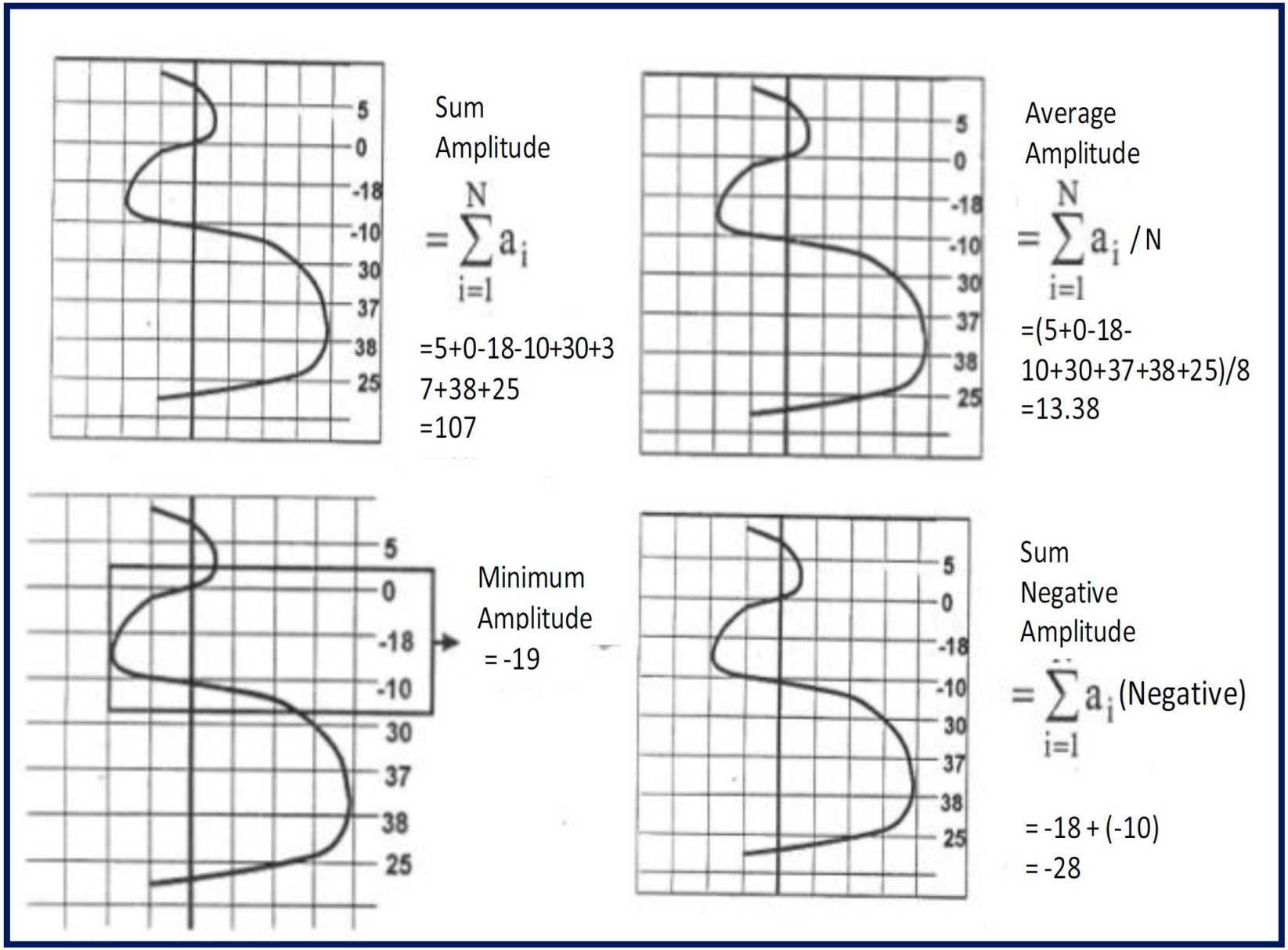

Figure 4. Calculation of some seismic attributes used in this research. After Sukmono (2008).

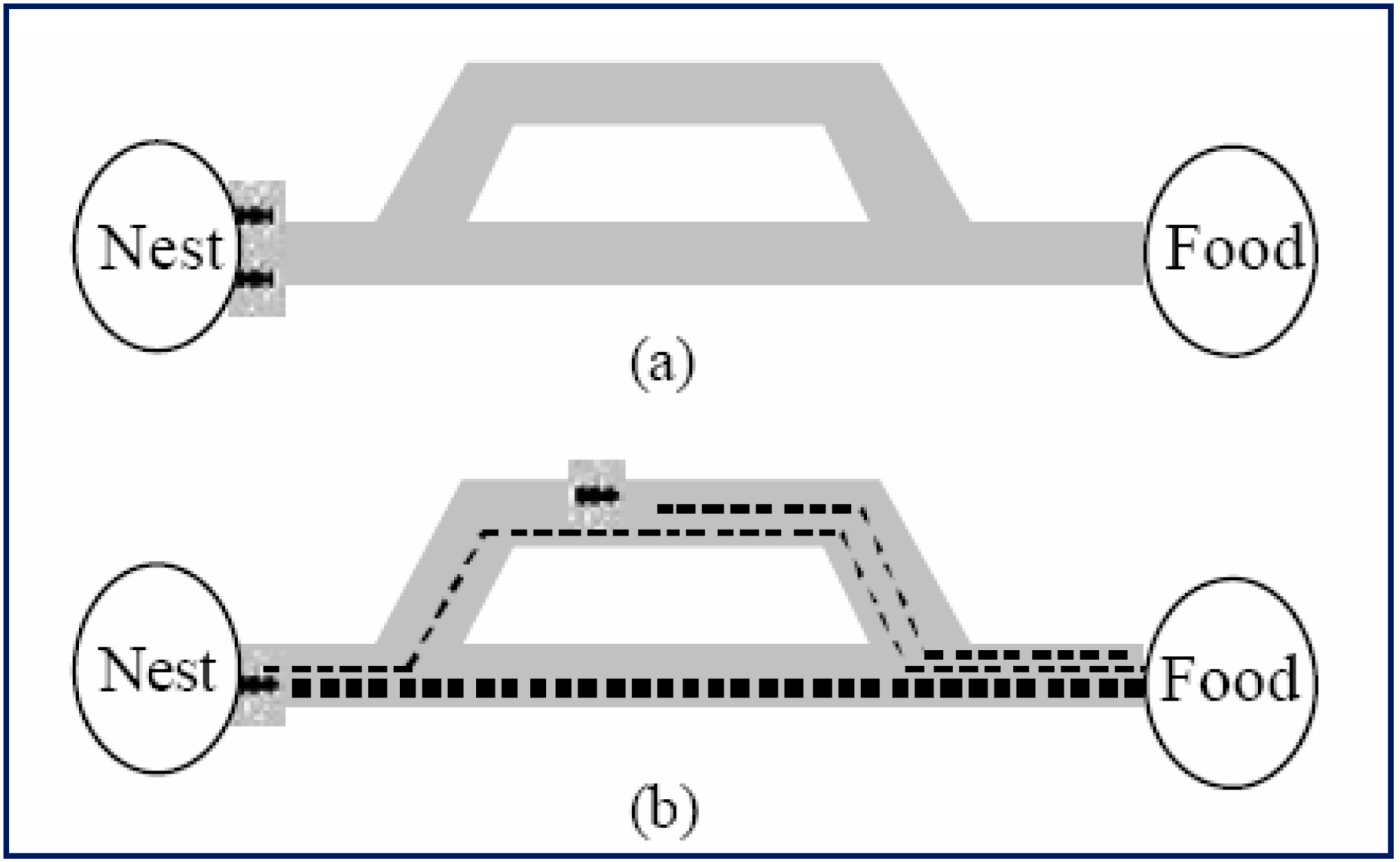

Figure 5. Schematic illustrating the principle of swarm intelligence which the Ant Tracker algorithm is based on. From Pedersen, (2002).

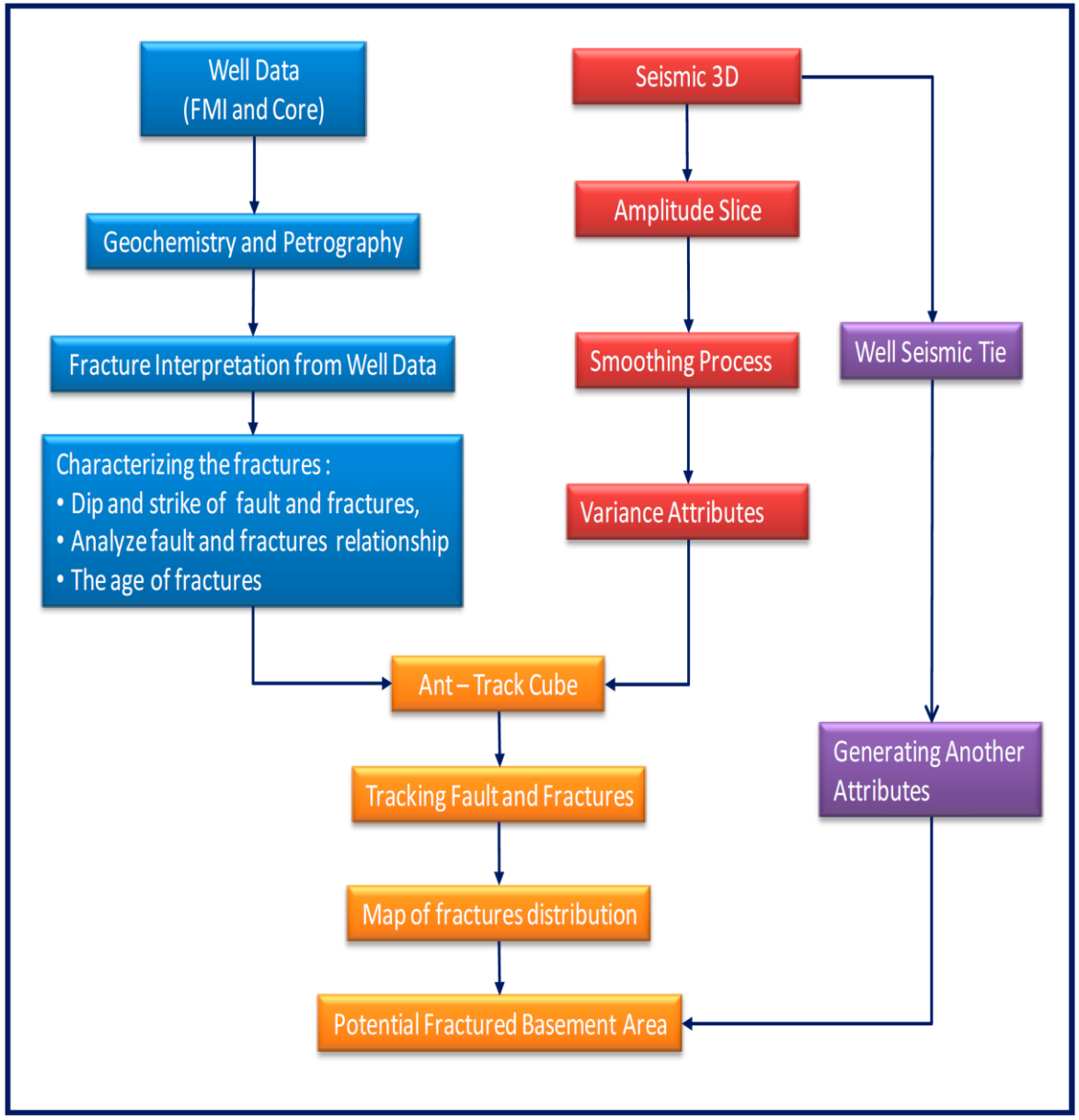

Figure 6. Workflow of this research.

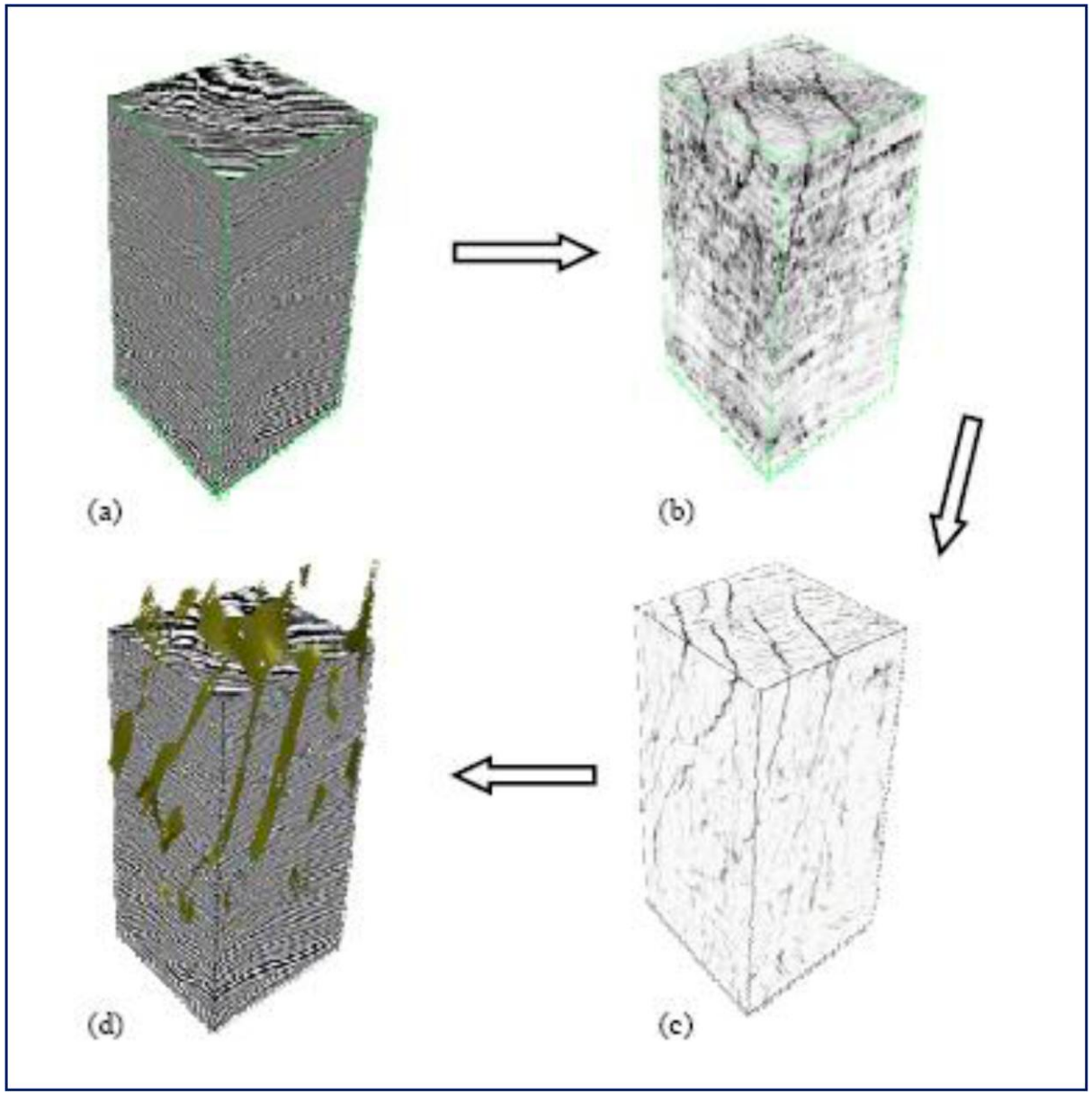

Figure 7. Schematic illustrating the Ant Tracking workflow. A variance cube (b) is generated from a seismic cube (a). Conditioning by Ant Tracking is applied and the faults are enhanced in the Ant Tracker cube (c). The fault surfaces are extracted and displayed as 3D fault patches (d). From Pedersen (2002).

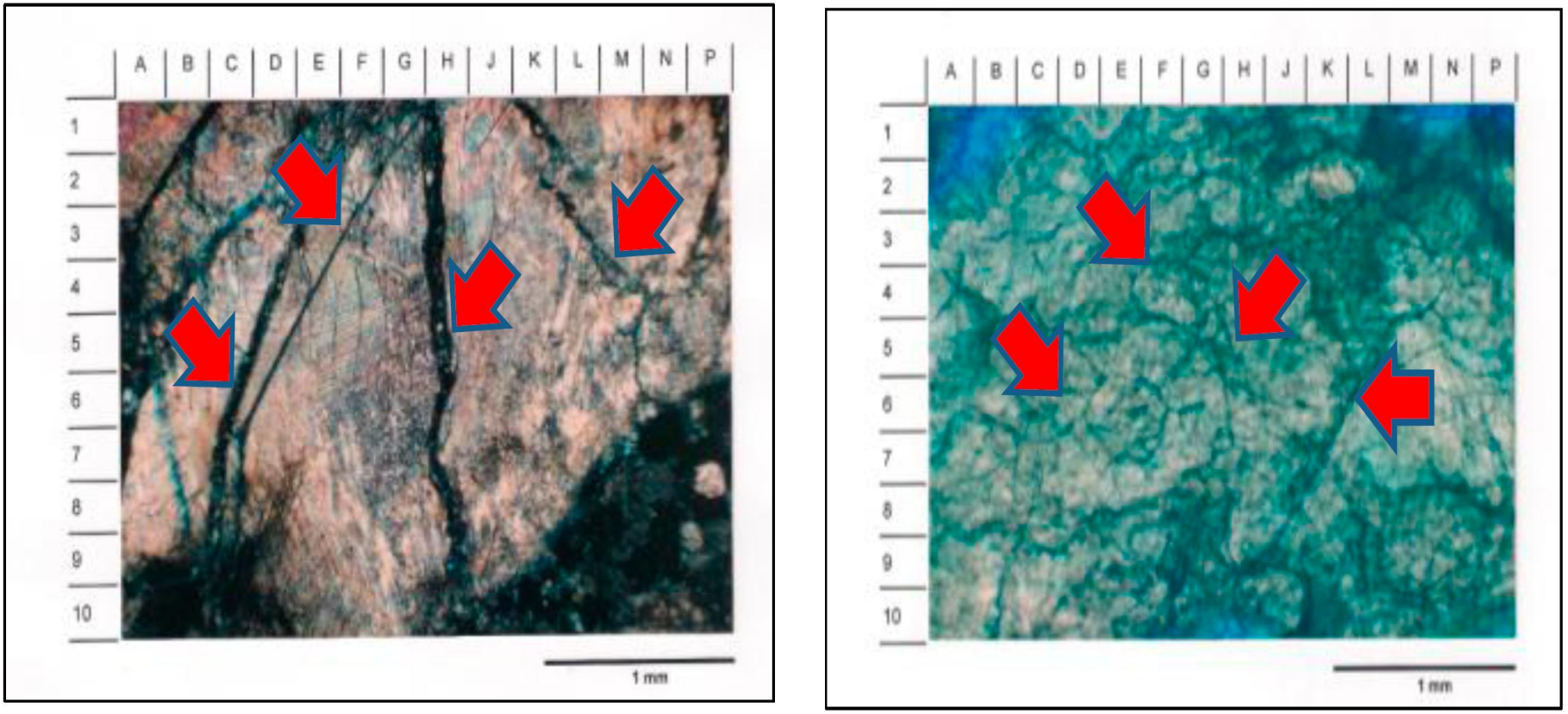

Figure 8. (Left) SEM of side wall core taken from MD-01 well at depth 2862 m. (Right) SEM of cutting from MD-02 well at depth (2745-2735 m). Red arrows shows fracture developments on both samples.

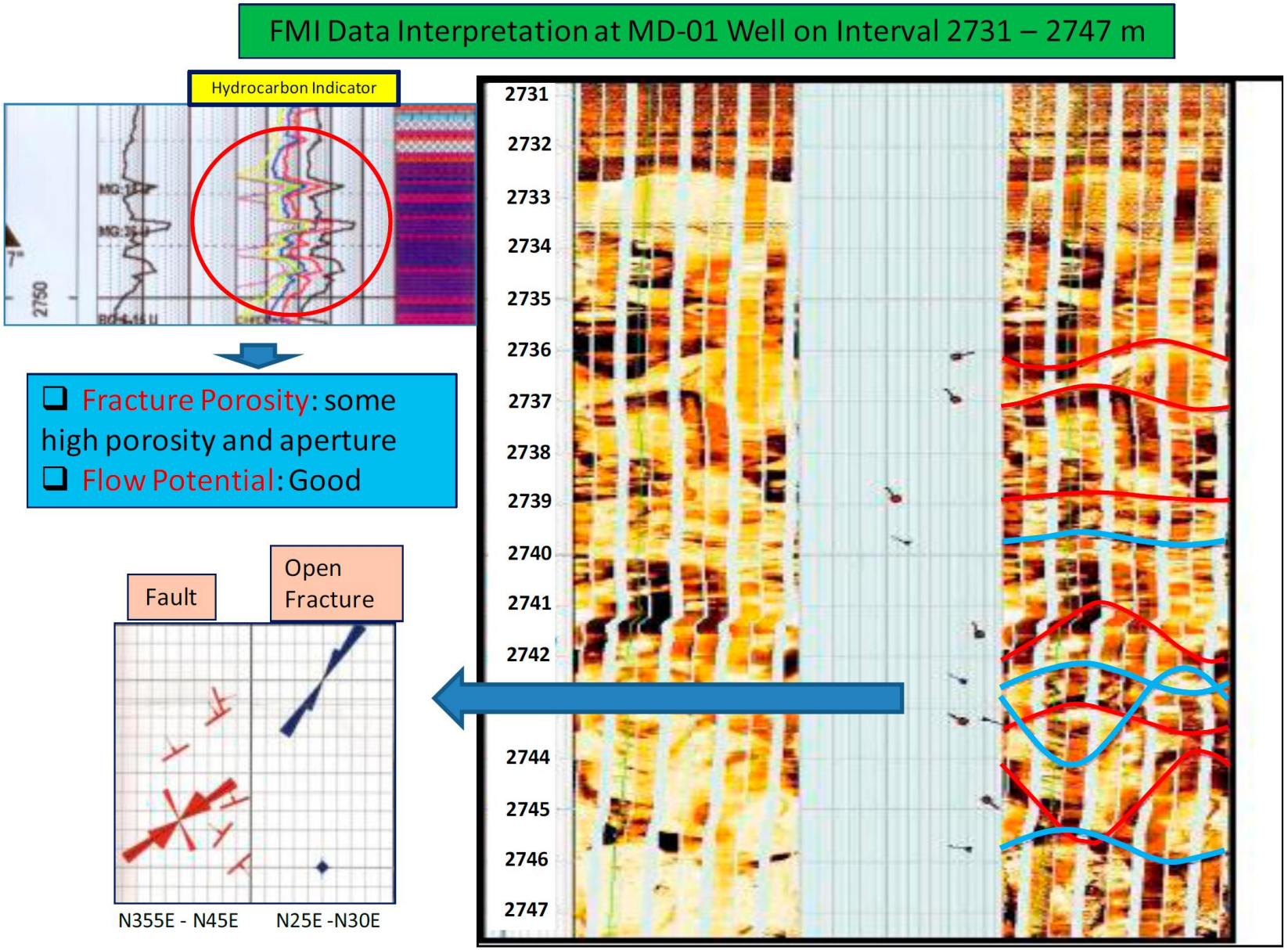

Figure 9. (Top Left) Master Log shows oil traces at this interval, which are inside the red circular line. (Right) Interpretation from FMI image: interpreted faults are showed by red solid curved line, and interpreted fractures are showed by blue solid curved line. (Bottom Left) The orientation of fault and fractures from this interpretation.

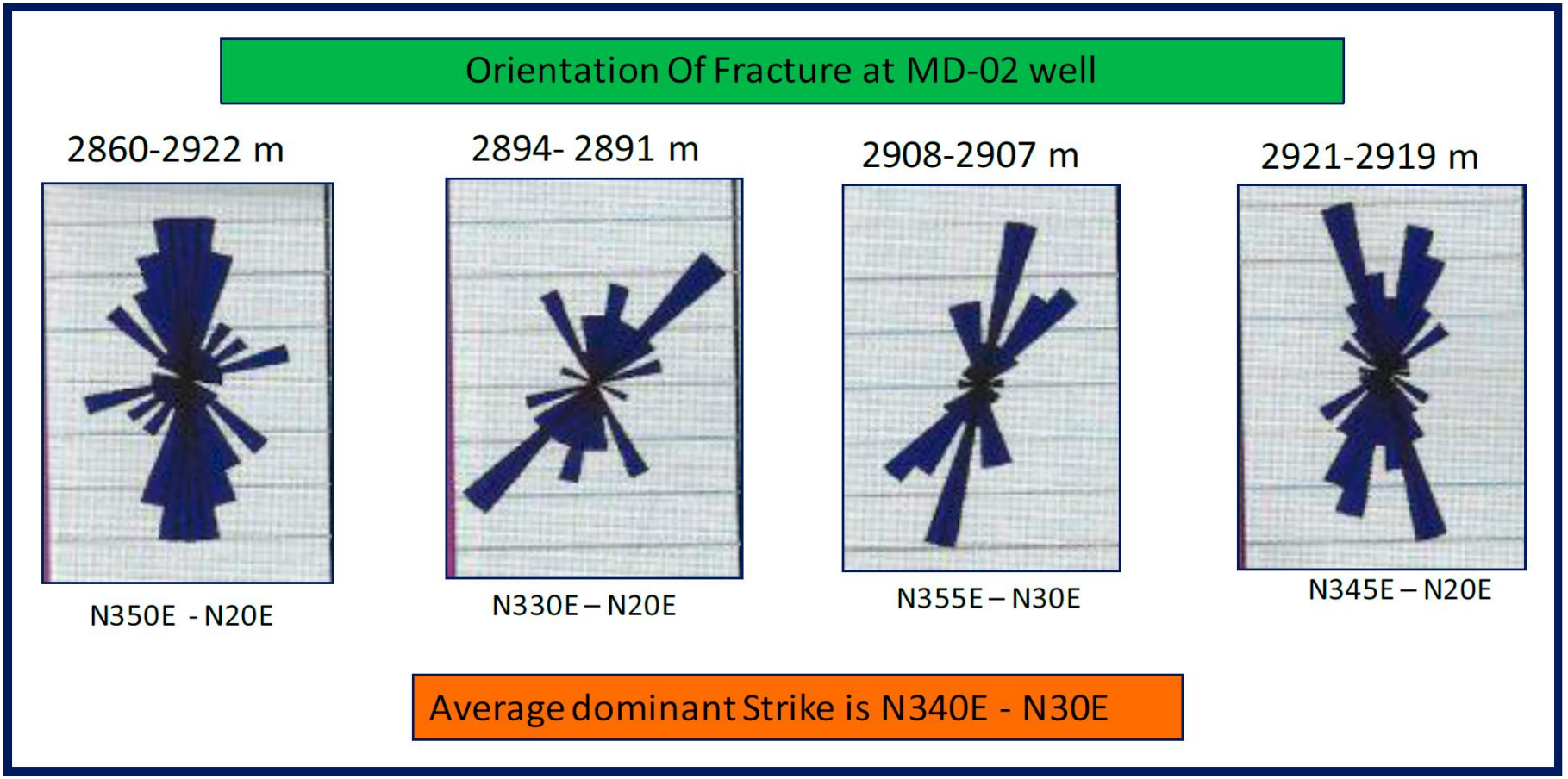

Figure 10. The orientation of conductive fractures (open fractures) at different depth intervals in MD-02 well. Average dominant strike of open fractures is N340E-N30E.

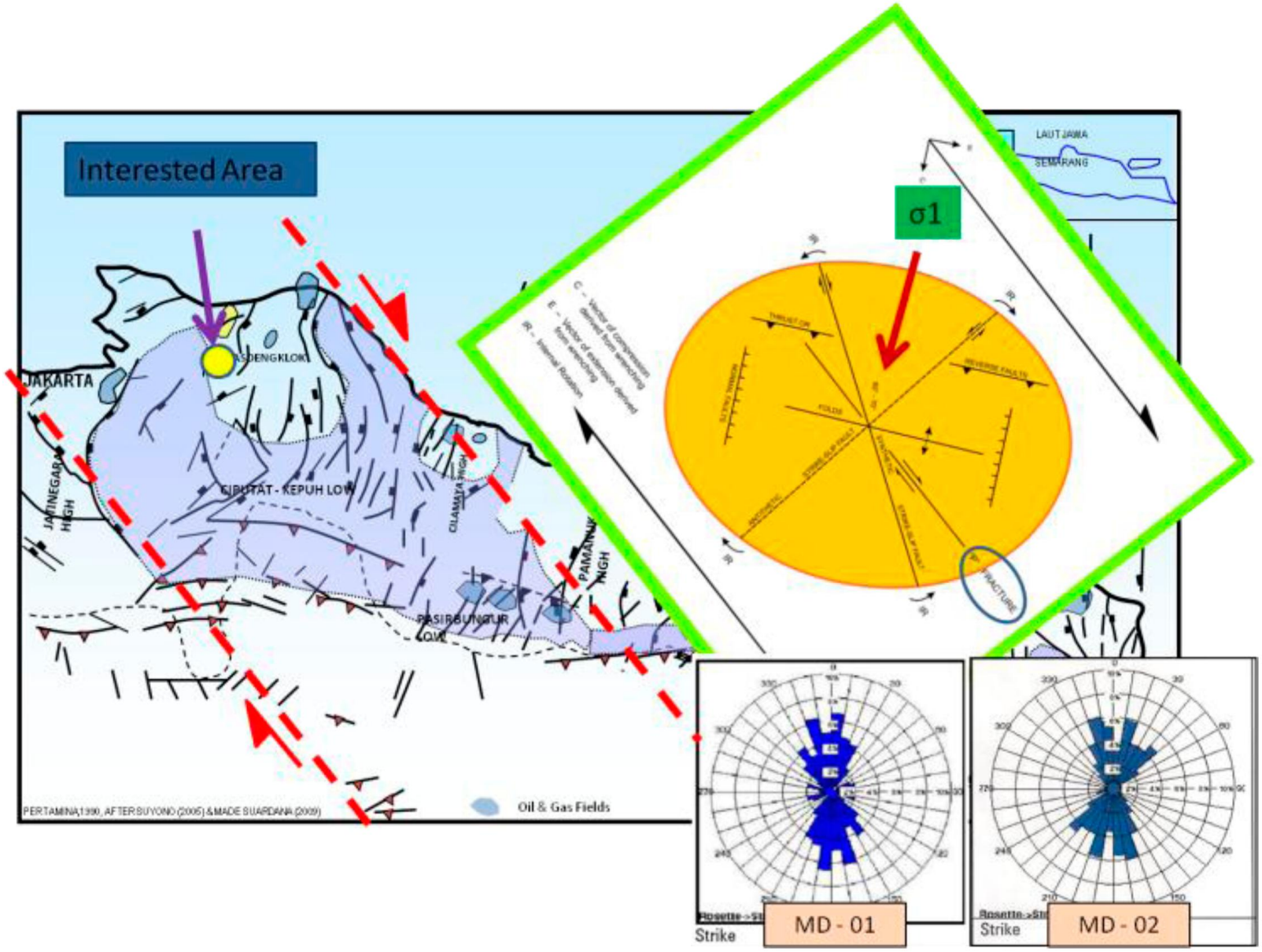

Figure 11. Reconstruction of regional stress (σ1) from fractures orientation. The regional stress field has created a strike-slip fault system that formed the pull-apart basin in this area.

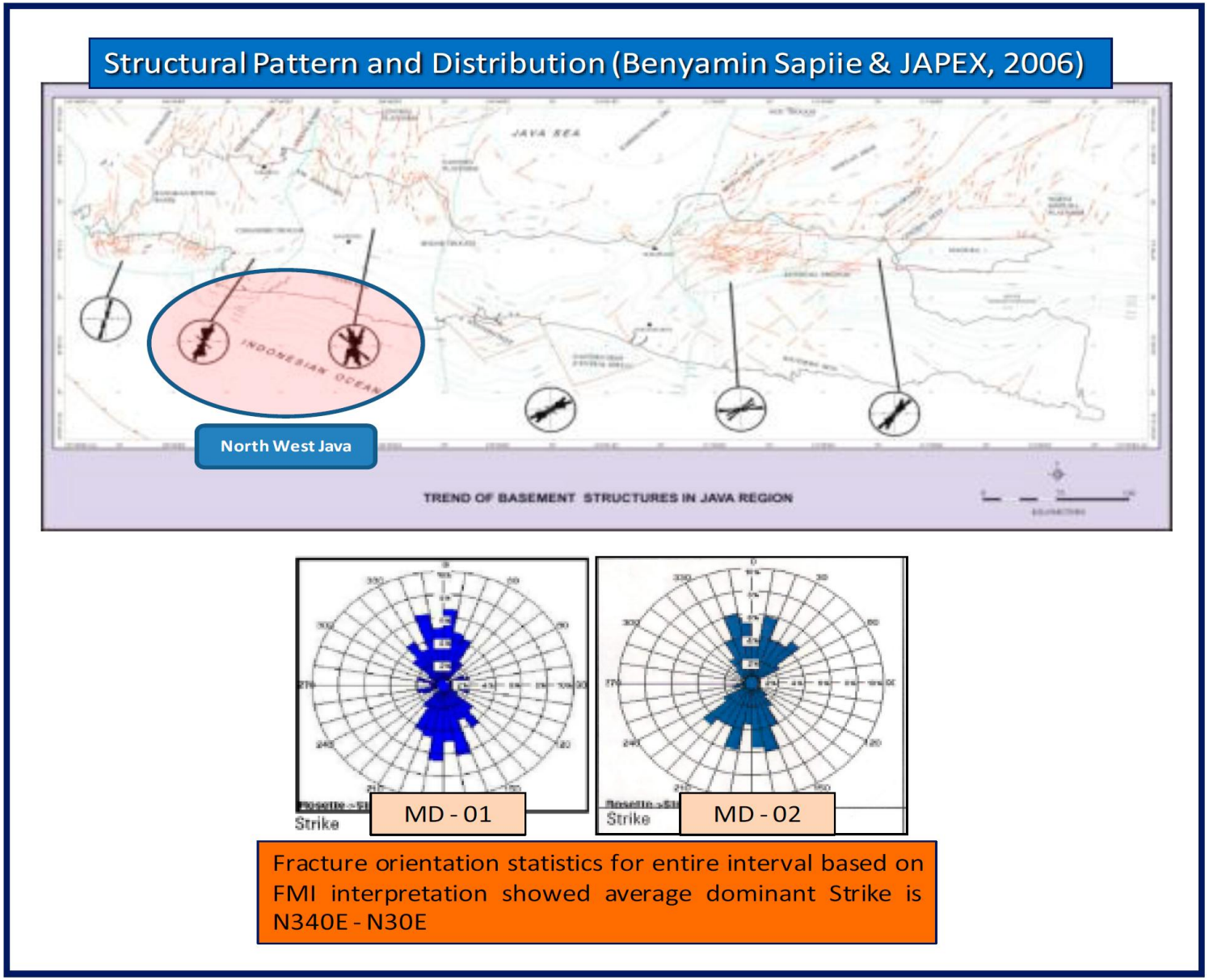

Figure 12. (Top) Structural pattern and distribution of fractures, after Benyamin Sapiie and JAPEX (2006); Northwest Java is shown inside the blue circular line. (Below) Fracture orientations for the entire basement rock interval in MD-01 and MD-02 wells based on FMI interpretation. Sapiie's map and FMI interpretation are correlated to each other.

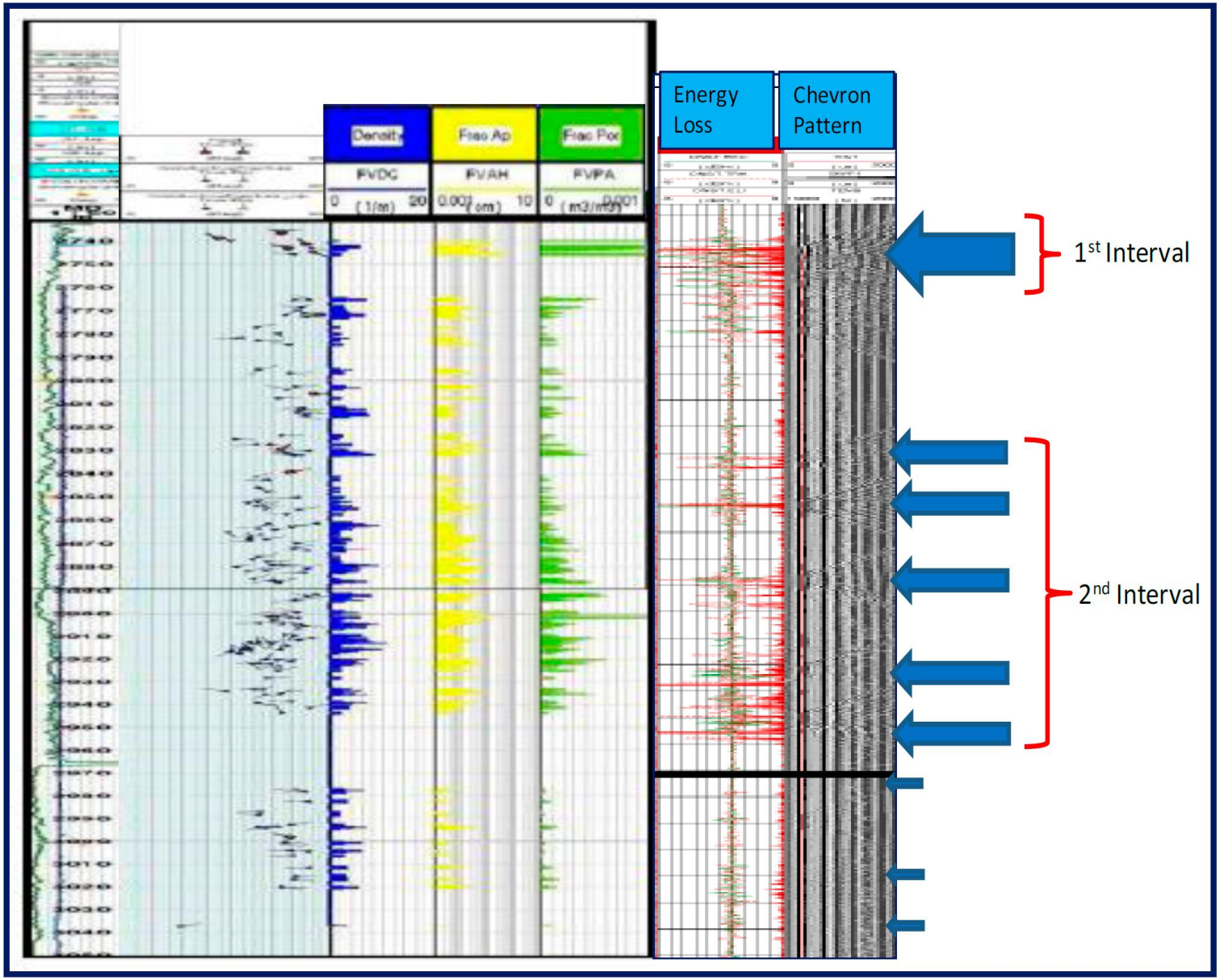

Figure 13. DSI Stoneley result: potential fractures are characterized by high fracture porosity, high energy loss and chevron pattern indication. The potential fractures are showed by blue arrow (larger blue areas indicate better potential fractures). Two potential intervals are drawn from this interpretation.

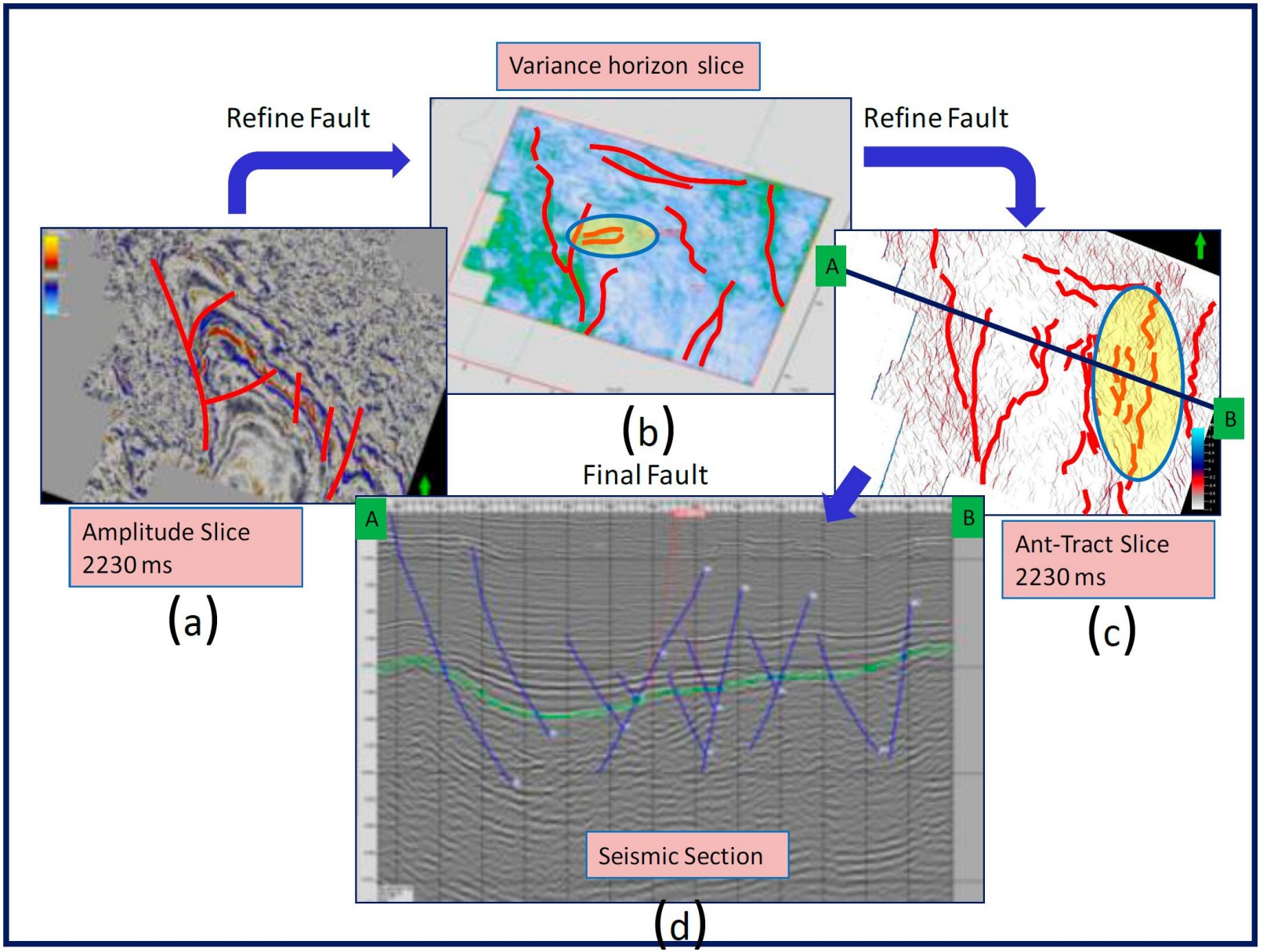

Figure 14. The process of generating fault maps using the different methods of (a) Amplitude Slice, (b) Variance Horizon Slice, new faults are seen and shown in the blue ellipse, and (c) Ant Track Slice, more faults are explicitly seen and shown in the blue ellipse. (d) Seismic section across path A-B with the final fault interpretation.

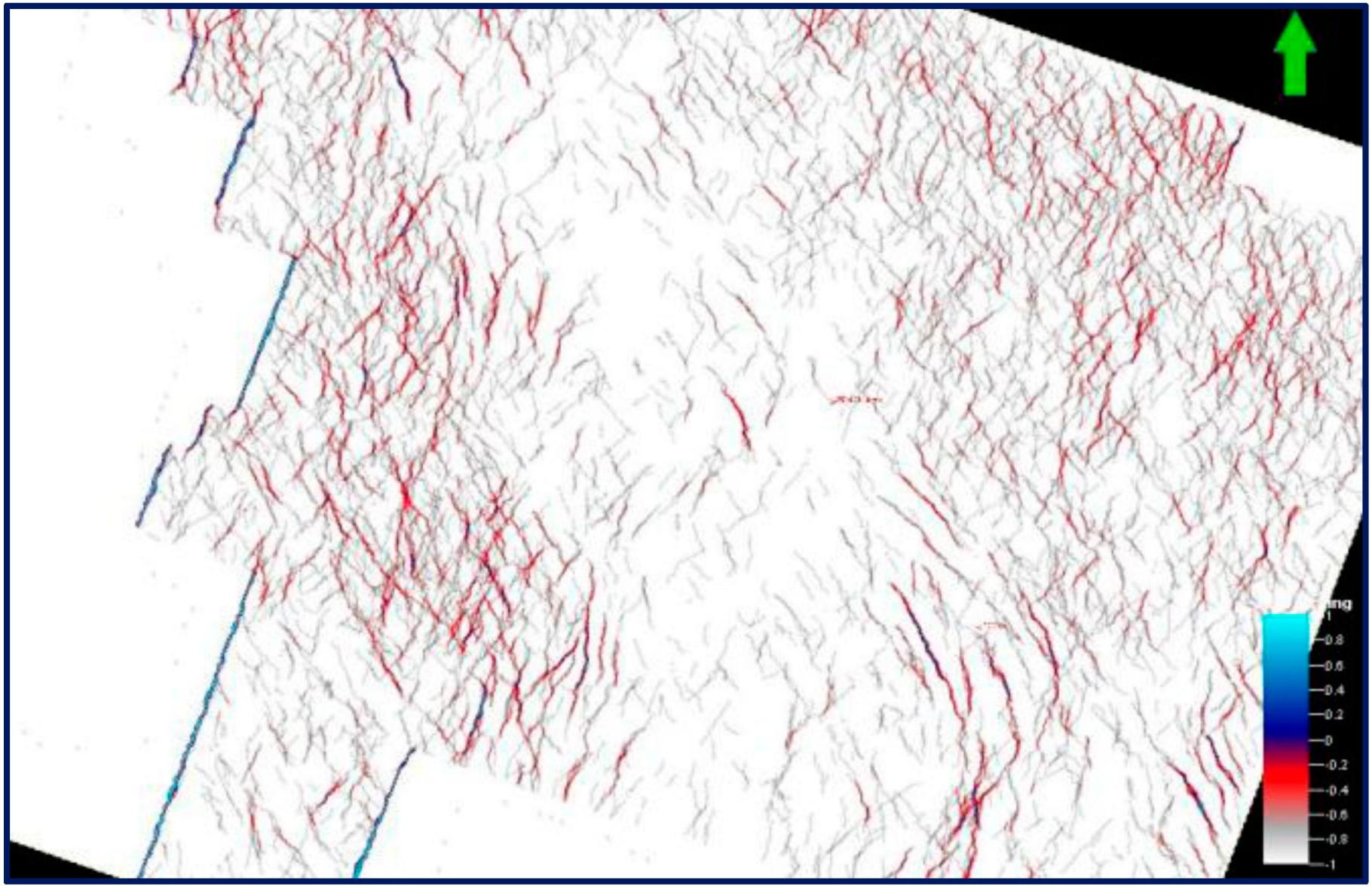

Figure 15. Ant Track map slices at 2230 ms. Strike of faults are from NNW-SSE to NNE-SSW, but dominantly in the north-south direction, and fracture orientations are from NNW-SSE to NNE-SSW.

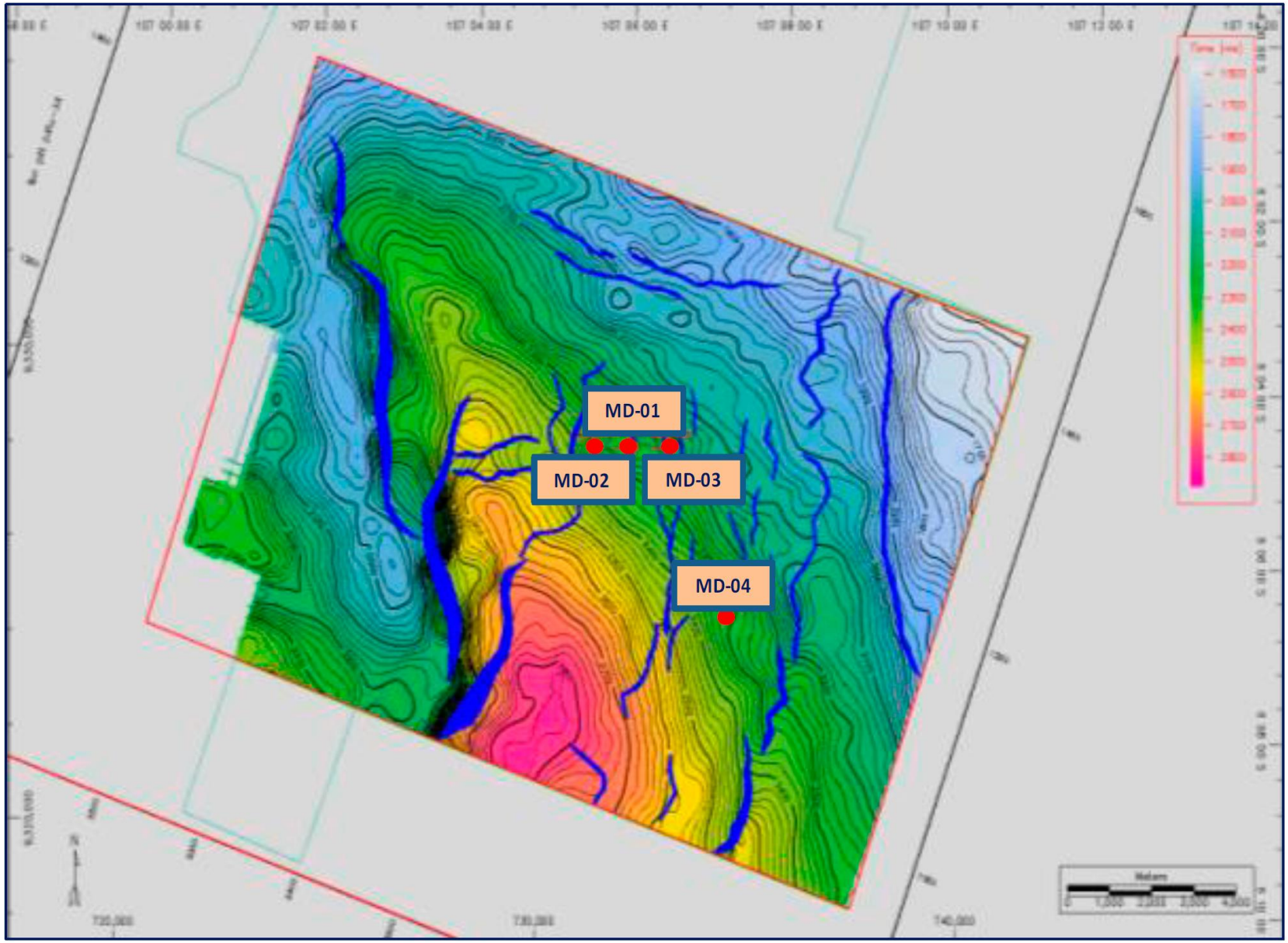

Figure 16. Time structure map of top of basement.

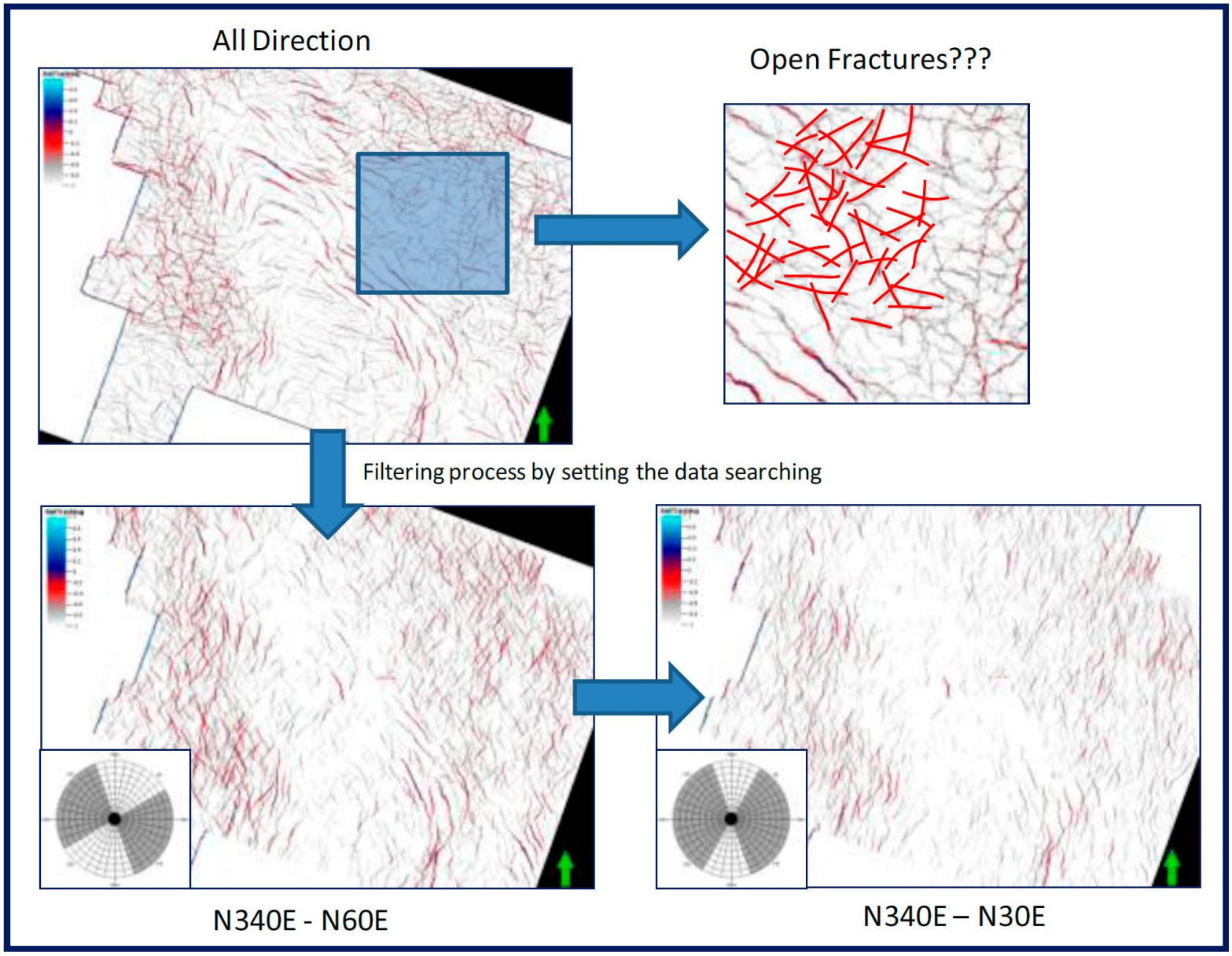

Figure 17. Filtering process to obtain open fractures distribution on the Ant Track map slice.

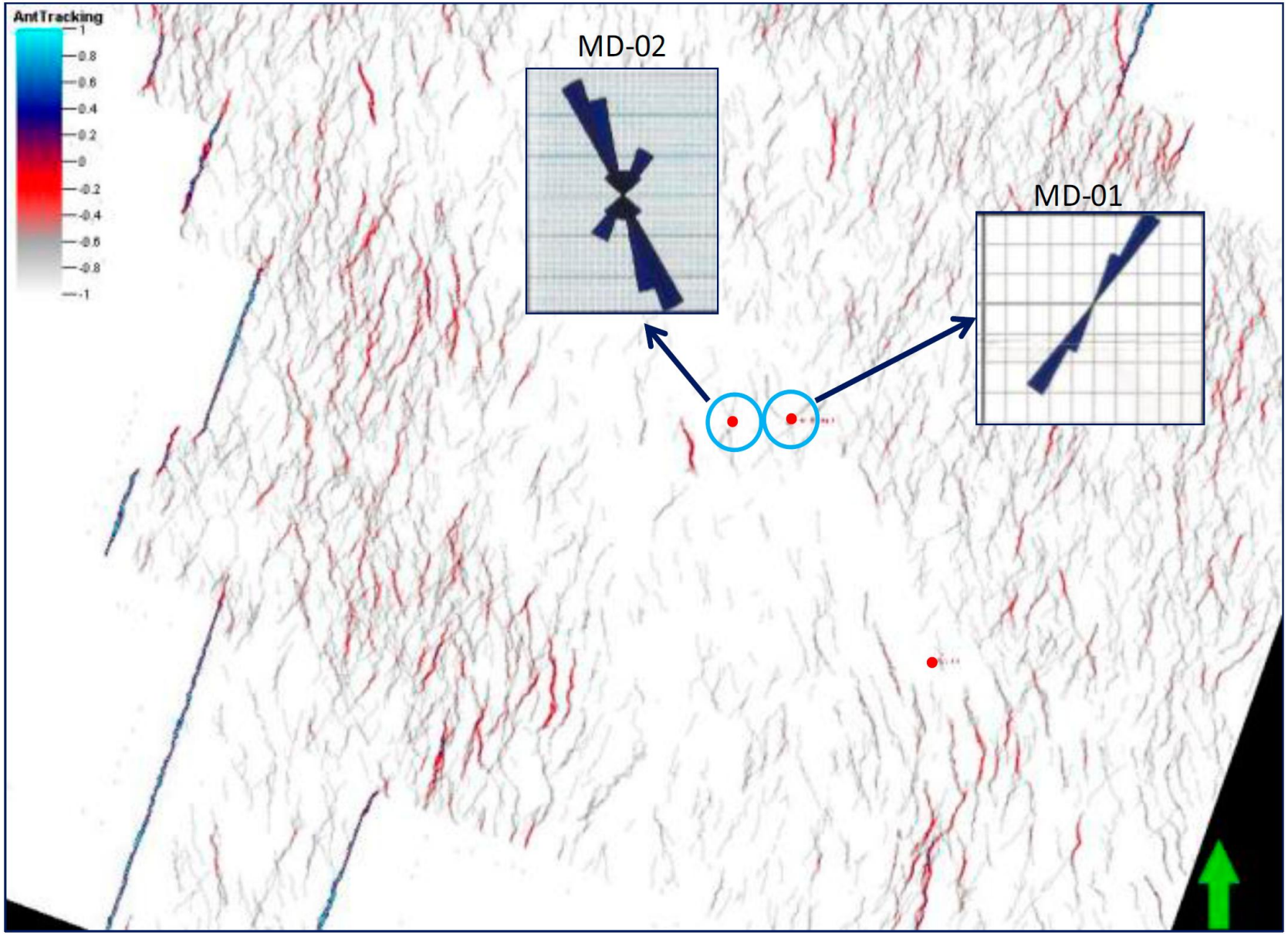

Figure 18. Ant Track map slice at 2230 ms. The map has a good correlation with FMI data from MD-01 and MD-02 wells.

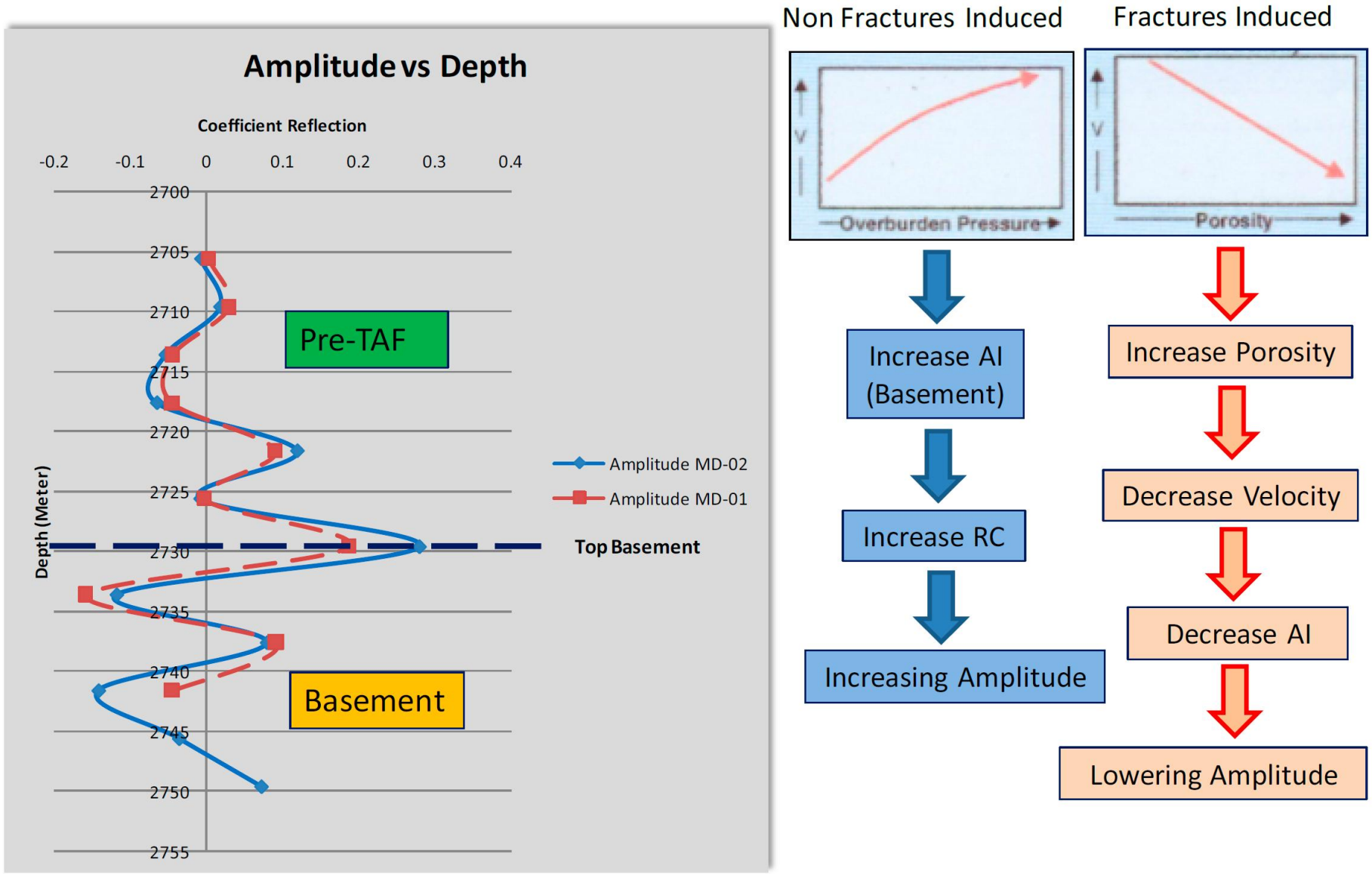

Figure 19. (Left) Petrophysical model represents the amplitudes changes from Pre-TAF to basement (marble). (Right) Hilterman (2001) draws the relationship between velocity with overburden pressure and porosity.

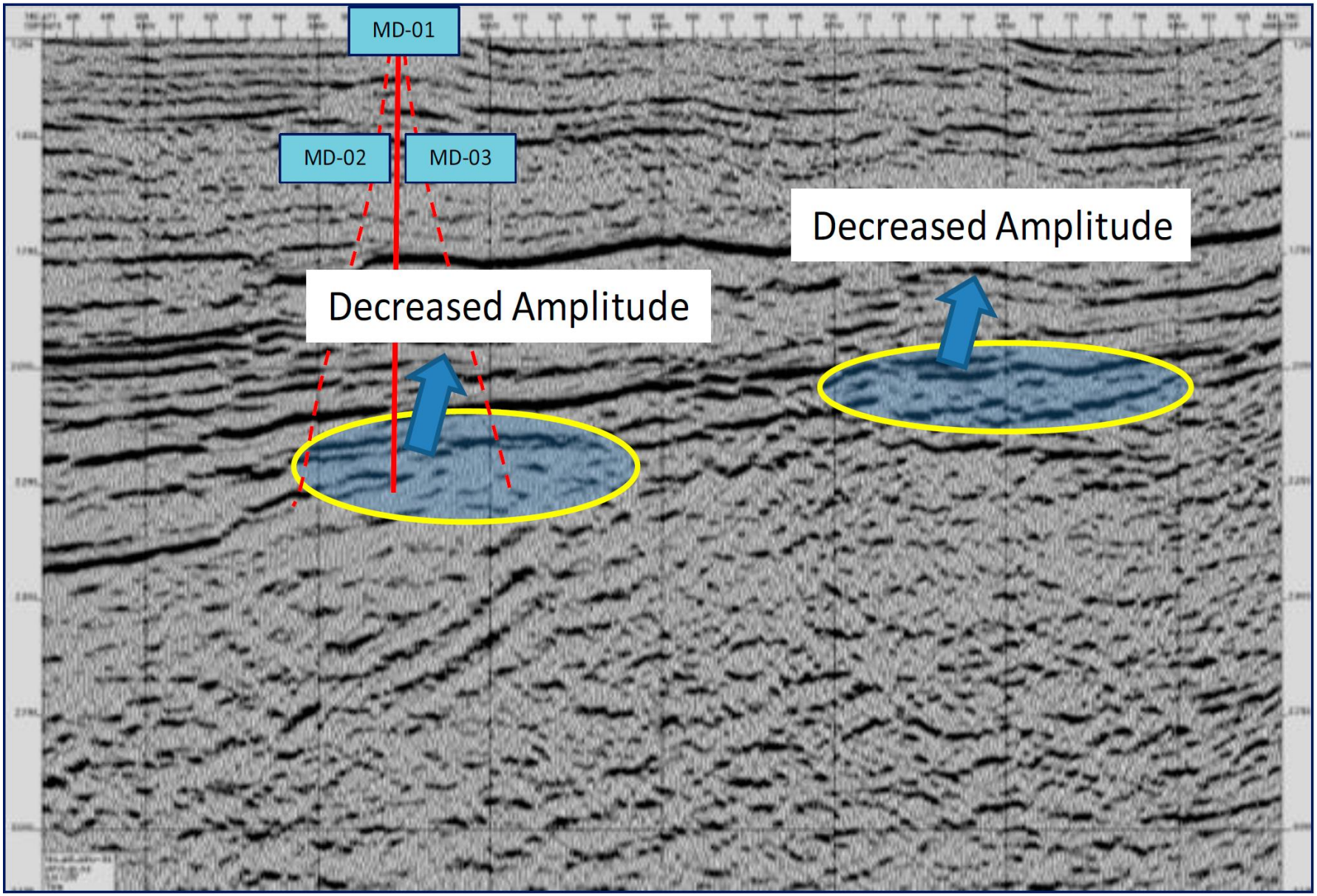

Figure 20. The anomaly of decreased amplitude at top of basement is showed in seismic section, which indicates many fractures developed there.

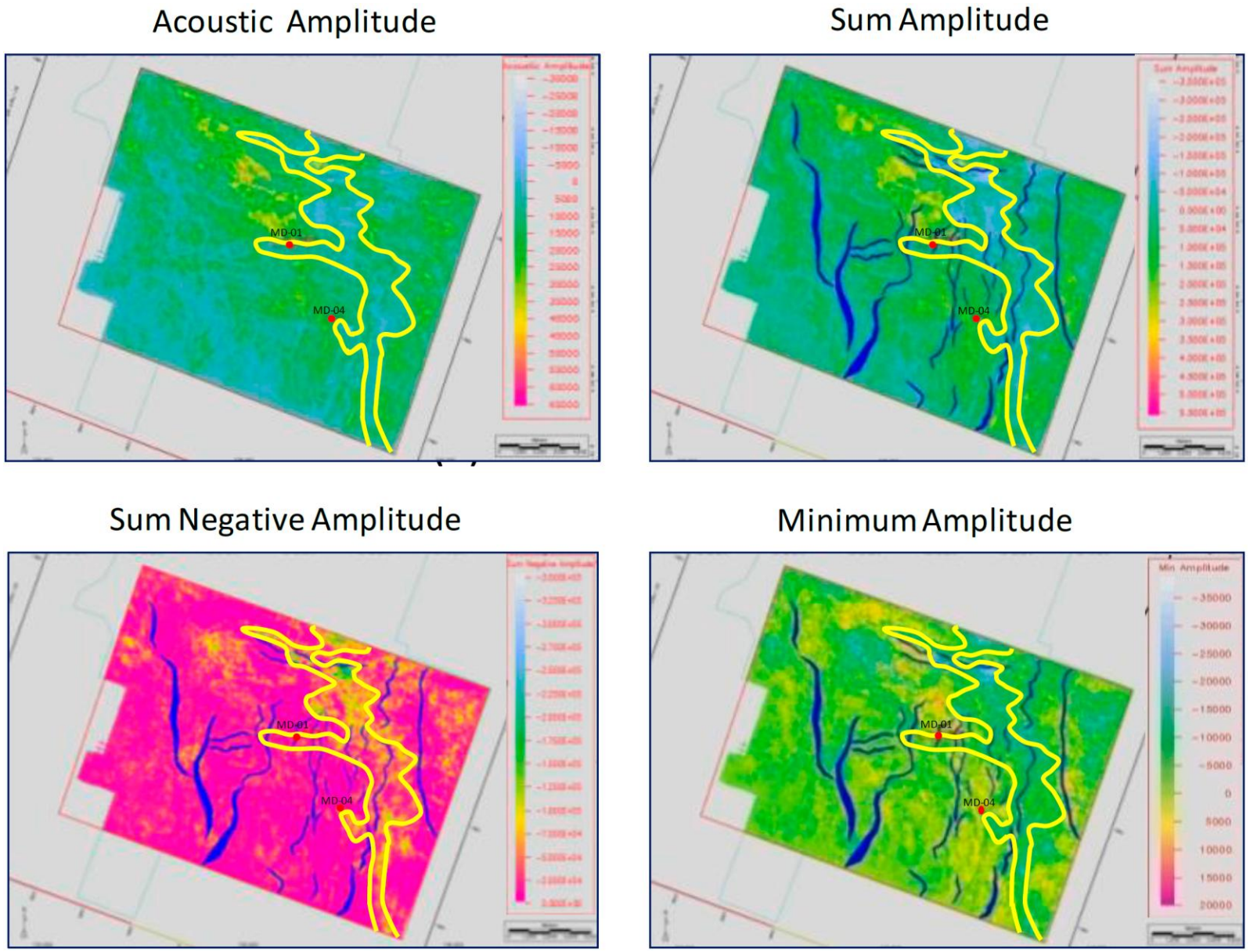

Figure 21. The lowest amplitude on each map represents high porosities related to the distribution of the first interval (potential fractures). The distribution of potential fractures is delineated by the yellow solid line.

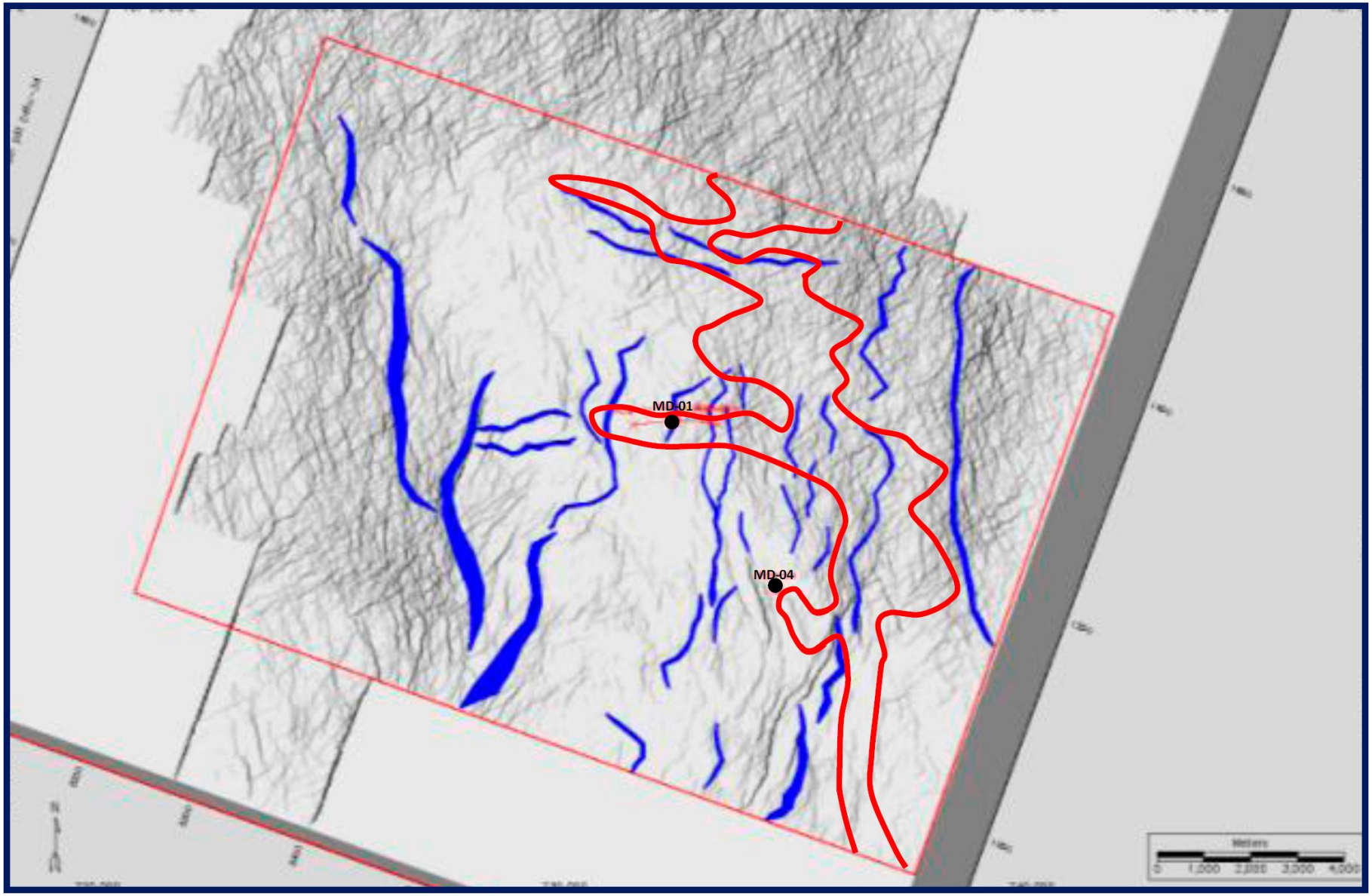

Figure 22. Distribution of first interval that contains potential open fractures (bounded by red solid line) from attributes analysis overlain on Ant Track map.

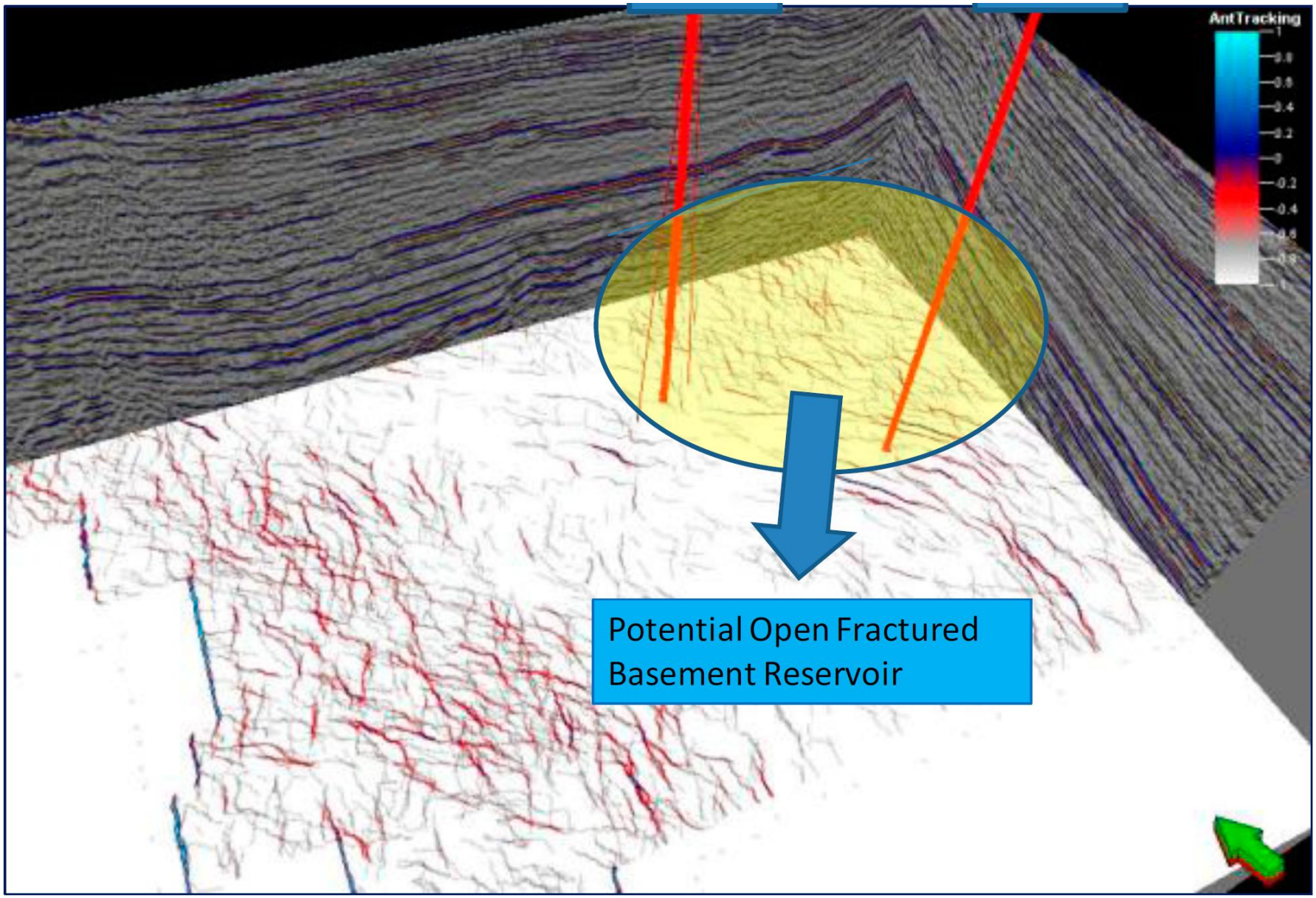

Figure 23. 3D view of potential open-fractured basement reservoir. Potential fractured basement reservoir is indicated to the northeast of MD-01 well.

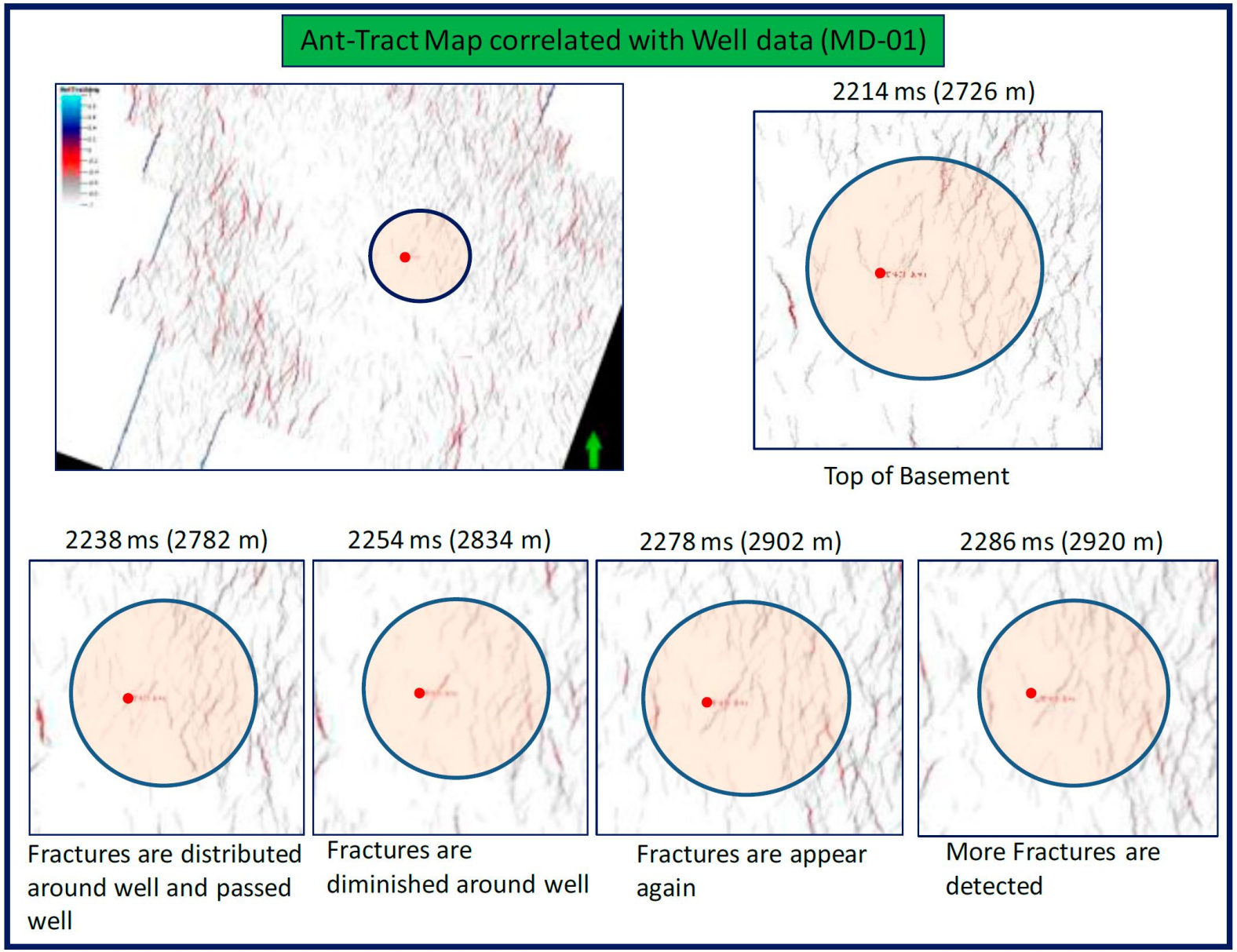

Figure 24. Ant Track maps sliced at different depths in well MD-01 correlates nicely with well data from master log (wellsite data).

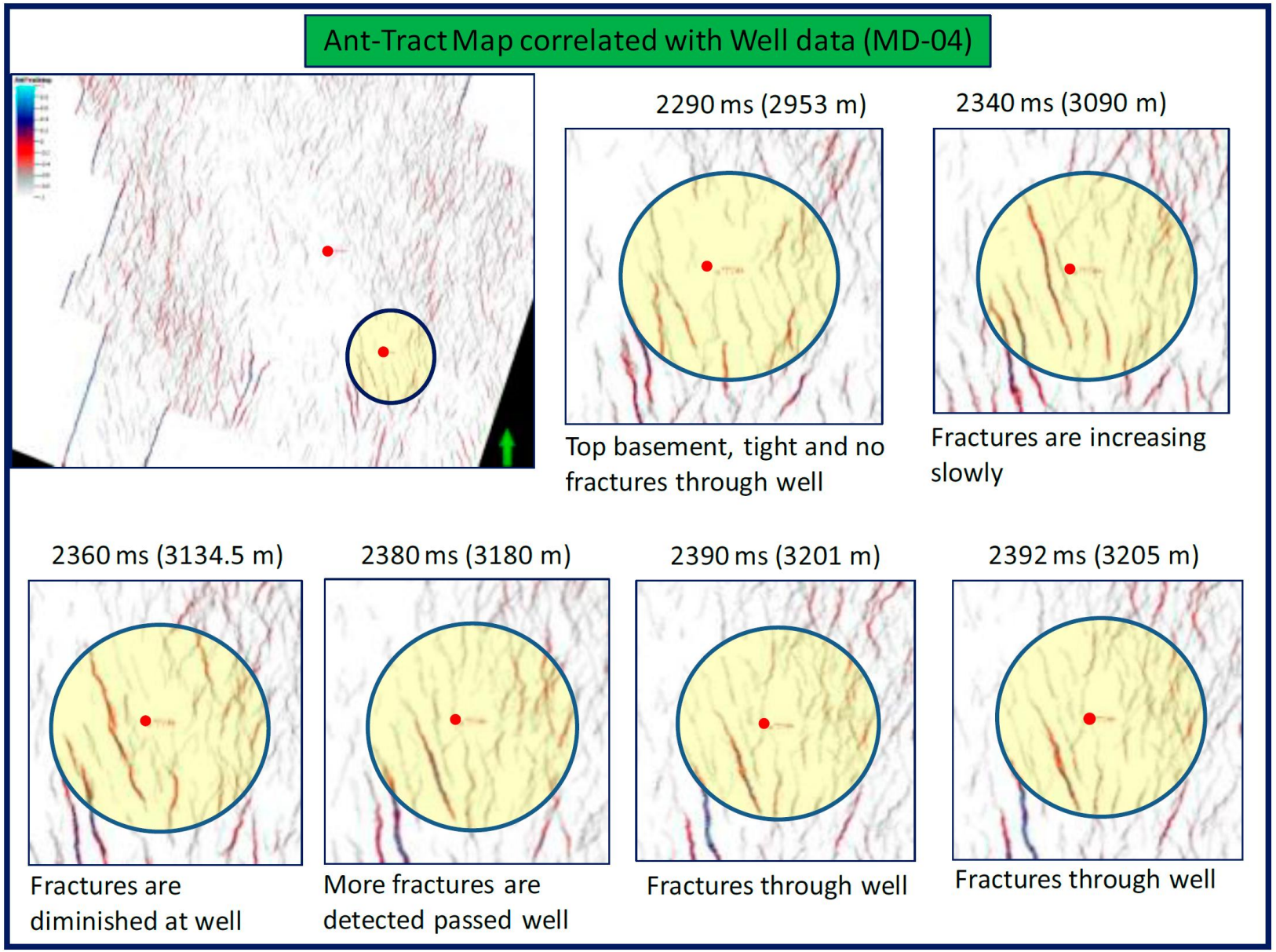

Figure 25. Ant Track maps sliced at different depths in well MD-04 correlates nicely with well data from master log (wellsite data).